Non-iterative algorithm for constructing self-energy matrix associated with open boundary conditions in 1-D systems.

D. Areshkin and C. White

Naval Research Laboratory, Code 6180, 1555 Overlook Ave, Washington, DC 20375

ABSTRACT

We present exact non-recursive method for constructing self-energy matrixes, which account for the contacts between quantum system and one-dimensional leads. Leads must possess chiral or translational symmetry, in all other respects their structure is arbitrary. Self-energy is constructed from the Green's function for the infinitely long perfect lead. Integral expression for the Green's function is replaced by the summation of the residues in the upper complex *K*-plane. Positions of the poles are obtained by using transfer matrix technique presented in the next article of this issue. The self-energy matrix is expressed as analytic function of the transfer matrix eigenvalues and eigenvectors. Such analytic form allows clear insight for the conductance expression based on non-equilibrium Green's function formalism. Case study examining the influence of random distortion on the localization length in nano-tubes demonstrates the utility of the method. Simple approximate analytic expression for the localization length provides a good fit to the simulation results, allowing better understanding of scattering processes in disordered systems. The algorithm is formulated for an orthogonal basis set, but no obstacles are foreseen in expanding it towards a non-orthogonal basis.

I. INTRODUCTION

Every quantum electronic device is connected to the outside world through the electric contacts. In the present paper we consider the case when the contacts have the form of one-dimensional leads with chiral or translational symmetry. Such leads may be, but not limited to silicon wires, organic molecules, or nano-tubes. Usually simulation of electronic device requires the detailed description only for the region where electron scattering and hence voltage drop occur. In the following we designate such region as the "system". If the lead outside the system can be considered perfectly periodic, its influence on the system may be substituted by the energy dependent self-energy matrix $\Sigma[\varepsilon]$. Such substitution does not involve any approximations and is mathematically exact. At the same time the use of self-energies is of great advantage because it limits the computation to finite size matrixes associated with the system alone. Given the contact self-energies and system's Hamiltonian it is straightforward to compute the Green's function of the system. Both the Green's function and the self-energy are the key quantities in non-equilibrium Green's function formalism (NEGF). The latter is a general tool for computing electron density, currents or current density, scattering matrixes for currents or separate wave functions, etc. However, despite of the mandatory presence of self-energy in any open-system calculations, the methodology for its computation is still incomplete. According to the recent reviews[1,2] there are two major approaches for self-energy computation. These two groups can be denoted as "iterative" and "transfer matrix" methods. The first group is based on the iterative solution of Eq.(12).[3-5] It is easy to prove (Appendix A) that the iterative solution of Eq.(12) does not converge for any *real* energy value corresponding to the *non-zero* density of states in the lead. Therefore to achieve the convergence of Eq.(X) or any variant of iterative algorithm originating from it, a finite imaginary part must be added to the energy. The iterative methods have two major drawbacks. The first one is the computational speed: iterative methods are slower[6] than transfer matrix methods. The second inconvenience is a small imaginary part, required for convergence. If $\mathrm{Im}[\varepsilon]$ is too small, the numerical error of the recursive method may ruin the computation. That is most likely in the vicinity of the band edge, where the self-energy of 1-D system is discontinuous. On the other hand finite $\mathrm{Im}[\varepsilon]$ is always a source

of systematic error. Therefore for each particular system the appropriate Im[ε] should be chosen individually through monitoring the convergence and precision of the recursion algorithm.

Transfer matrix methods[6-10] are exact and computationally efficient. They stem out of the works by Allen[8], Lee, and Joannopoulos[9], who have developed computation methods for the surface Green's functions. The later work by Umerski[6] provides a novel outlook to the surface Green's function construction through the Möbius transformation. Usually the Umerski's method is not ranked among the transfer matrix methods. However, despite its formal uniqueness, this method utilizes essentially the same transfer matrix as the earlier works.[9,10] The transfer matrix class of algorithms builds the Green's function and hence the self-energy from the solutions of the problem $H[\Lambda_i]\cdot C_i = \varepsilon\, C_i$; $\Lambda_i \equiv Exp[i\,K_i]$. Here $H[\Lambda_i]$ is the Hamiltonian of the perfect lead defined by Eq.(5) and Fig. 1(b), and $\{K_i\}$ and $\{C_i\}$ are the sets of all possible wave numbers and wave functions, which satisfy this equation for a *given* ε. The sets $\{K_i\}$ and $\{C_i\}$ are obtained as the eigenproblem solution for the transfer matrix.

The major drawback of the transfer matrix methods, which is avoided by iterative algorithms, was the inability to handle problems with the singular coupling matrix τ (Fig. 1(b)). The first attempt to resolve this issue has been undertaken by Chang and Schulman.[10] Their method was formulated for the special type of singularity inherent to the coupling between crystalline planes. That was not considered a deficiency of the method, because it was adequate for the physical problem in hand. However, with the advent of 1-D quantum wires, this shortcoming became noticeable, since the singularity structure of the coupling matrix associated with 1-D Hamiltonian does not generally match any regular pattern and cannot be handled using the Chang and Schulman's algorithm. This issue has been recently addressed by Tomfohr and Sankey who have developed the transfer matrix technique for an arbitrary singular τ.[11] This technique, however, has inherent numerical instability problem. It restricts the usage of Tomfohr-Sankey's method to small τ matrixes and (or) simple Hamiltonians with few energy bands confined within moderately small energy range.

In the present paper computation of the Green's function follows the same intuitively straightforward path, which has been initially suggested by Allen.[8] The advance-

ment of our method includes "fixes" for the two principle drawbacks of the original Allen's approach. Firstly, even if the sets $\{K_i\}$ and $\{C_i\}$ are assumed to be known, Allen's method is still not suited for Green's functions computation if the coupling matrix τ is singular. Secondly, Allen's expression for the Green's function is not analytic and hence cannot be extended into complex energy plane, which is essential for contour integration. We also propose the new method for the construction of the transfer matrix to obtain $\{K_i\}$ and $\{C_i\}$. The proposed method is faster and more stable numerically than the Tomfohr-Sankey's algorithm. It is capable of handling the systems with singular coupling Hamiltonian sub-blocks for which the Tomfohr-Sankey's method fails. The set of the systems handled by the Tomfohr-Sankey's method is the subset of the systems handled by our method. Since the transfer matrix algorithm has stand-alone value and its applicability is not restricted to the Green's functions and self-energies of 1-D leads, we present it in the form of the separate article, which follows the current paper. In both papers we assume orthogonal basis set.

When a random distortion is imposed on the ideal quantum wire, it can be statistically characterized by the two length parameters: L_p and L_φ.[12] The former is the momentum scattering length: when the distorted region becomes larger than L_p, the conductance becomes appreciably different from its ideal value due to backscattering. The latter is the phase scattering length: if the separation between two points is larger than L_φ, the phases of the wave function at these points become independent from each other. At low temperatures, when the phonon scattering is negligible, $L_\varphi >> L_p$. If the length of the distorted region L satisfies the condition $L_\varphi > L > L_p$, the conductance dependence on L can be approximately described as $C[L]=C_0 Exp[-L/L_0]$. Here C_0 is the value of the ideal conductance, and parameter L_0 is called the "localization length". We apply the self-energy computation algorithm to the evaluation of L_0 in two ways: numerically and analytically. The numerical evaluation of L_0 is performed by statistical averaging of $Log[C[L]]$ over the ensemble of randomly distorted nano-tubes. The obtained numerical result fits well the approximate analytical expression for L_0. The latter was obtained using the concept of the complex K-states - the foundation of the Green's function and self-energy computation method.

To facilitate the understanding of the self-energy computation algorithm we introduce it for the simplest case when the translationally symmetric 1-D system is described by the tri-block-diagonal Hamiltonian. Extension to the multi-block-diagonal Hamiltonians and screw symmetry is performed afterwards. The paper is structured in the tutorial format: first the step-by-step algorithm for self-energy construction is introduced, after that the detailed explanation of each step is provided. The rest of the paper is organized as follows. The next section contains the problem description and the related definitions. Section III presents the algorithm for self-energy computation for the simplest tri-block-diagonal, translationally symmetric case. It contains all necessary information for those who don't want to delve into underlying theory and need "just the self-energy matrix" for the given energy value and Hamiltonian sub-blocks. Section IV relates self-energy matrixes to the Green's function sub-blocks of the infinite (not semi-infinite!) periodic 1-D structure. Section V provides the general expression for the arbitrary Green's function matrix element through the integral in K-space and explains how K-integration in the complex K-plane can be substituted by the residue summation. Sections VI-VII expand the algorithm onto general type multi-band-block-diagonal Hamiltonian and structures possessing screw symmetry. Section VIII contains the derivation for the approximate localization length expression and its comparison to the numerical results.

II. PROBLEM SETUP

In a localized basis representation the Hamiltonian associated with 1-D translationally periodic lead is represented by an infinite block-band matrix. The number of bands equals $2W + 1$, where $2W$ is the number of neighbor unit cells, which interact with any given unit cell. The example in Fig. 1(a) illustrates second neighbor approximation described by a five-band Hamiltonian matrix. The movement along linear system corresponds to the downward movement along the Hamiltonian diagonal. Even if the system has complex shape, e.g. spiral, we use notions "left" and "right" to denote the relative positions of the points in the system: the point corresponding to the upper-left sub-blocks of the Hamiltonian is said to lie to the left from the point, which corresponds to the bottom-right sub-blocks.

The minimal size of a self-energy matrix in an atomic orbital representation equals the interaction range. It is convenient to make all matrixes involved in the self-energy computation of the same size as the self-energy matrix. To implement this idea one needs to view band-diagonal Hamiltonian as a tri-block-diagonal matrix with the sub-block size equal to the interaction range. That means the size of the original minimal unit cell, which is based on the symmetry of the lead, must be increased by some integer factor to make the unit cell sufficiently large and thus to prevent the interaction beyond the nearest neighbors. Figure 1 illustrates the idea by joining two unit cells into one supercell and describing the Hamiltonian through the tri-block diagonal form. In the following, until section VI, the term "unit cell" refers to the "renormalized" unit cell associated with tri-block diagonal Hamiltonian. The self-energy matrix and the Green's function sub-blocks used in intermediate computations have the same dimensions as the sub-blocks of the tri-block diagonal Hamiltonian. In the following we use tri-block diagonal Hamiltonian as the standard description of 1-D periodic lead. We adopt the notation indicated in Fig. 1(b): h and τ describe respectively the interaction between the orbitals belonging to the same unit cell and to the nearest neighbor unit cells. The size of Hamiltonian sub-blocks h and τ is N.

The goal of the paper can be best explained by the example. Suppose that the perfect infinite lead contains single defect extending into three unit cells (Fig. 2). This aperiodic portion of the lead is described by the Hamiltonian sub-block H_D of the size $3N$. Suppose we need to compute Green's function sub-block G_D associated with H_D for energy ε. If the self-energy matrixes $\Sigma_L[\varepsilon]$ and $\Sigma_R[\varepsilon]$ describing the contacts to the left and the right portions of semi-infinite leads are known, the computation of the Green's function is trivial:

$$G_D[\varepsilon] = \left(I \times \varepsilon - H_D - \tilde{\Sigma}_L[\varepsilon] - \tilde{\Sigma}_R[\varepsilon]\right)^{-1} \text{, where} \tag{1}$$

$$\tilde{\Sigma}_L[\varepsilon] = \begin{pmatrix} \Sigma_L[\varepsilon] & 0 & 0 \\ 0 & 0 & 0 \\ 0 & 0 & 0 \end{pmatrix}, \text{ and } \tilde{\Sigma}_R[\varepsilon] = \begin{pmatrix} 0 & 0 & 0 \\ 0 & 0 & 0 \\ 0 & 0 & \Sigma_R[\varepsilon] \end{pmatrix} \tag{1-a}$$

The size of unity matrix I and matrixes $\tilde{\Sigma}_L[\varepsilon]$ and $\tilde{\Sigma}_R[\varepsilon]$ is $3N$. The size of matrixes $\Sigma_L[\varepsilon]$ and $\Sigma_R[\varepsilon]$ is N. Knowledge of G_D allows the immediate computation of electron density matrix at the defect region:

$$\rho = -\frac{2}{\pi}\int_{-\infty}^{\infty} \mathrm{Im}\left[G_D[\varepsilon]\right] \times f\left[\varepsilon - \mu_0\right] d\varepsilon \ . \tag{2}$$

Here f is the Fermi function, and μ_0 is the Fermi level, which is the same for both leads if the system is under equilibrium conditions. Integration in Eq.(2) is usually substituted by contour integration in the upper complex energy half-plane.[13] In the case when the Fermi level in the left and the right leads is shifted by respectively $\Delta\mu_L$ and $\Delta\mu_R$ by the applied voltage $\Delta V = \Delta\mu_L - \Delta\mu_R$

$$G_D[\varepsilon] = \left(I \times \varepsilon - H_D - \tilde{\Sigma}_L[\varepsilon - \Delta\mu_L] - \tilde{\Sigma}_R[\varepsilon - \Delta\mu_R]\right)^{-1} \ . \tag{1-b}$$

In that case the non-equilibrium density matrix, which imaginary part becomes non-zero and asymmetric, is[14]

$$\rho = -\frac{1}{\pi}\left(\int_{-\infty}^{\infty} f\left[\varepsilon - \left(\mu_0 + \Delta\mu_L\right)\right] G_D \cdot \mathrm{Im}\left[\tilde{\Sigma}_L[\varepsilon - \Delta\mu_L]\right] \cdot G_D^* \right.$$
$$\left. + \int_{-\infty}^{\infty} f\left[\varepsilon - \left(\mu_0 + \Delta\mu_R\right)\right] G_D \cdot \mathrm{Im}\left[\tilde{\Sigma}_R[\varepsilon - \Delta\mu_R]\right] \cdot G_D^* \right) \ . \tag{2-a}$$

The current between orbitals α and β is [15]

$$j_{\alpha,\beta} = -\frac{4e^2}{\hbar}\mathrm{Im}\left[\rho_{\alpha,\beta}\right] H_{D_{\alpha,\beta}} \ , \tag{3}$$

which is trivially transformed to the Landauer's expression for the total current:

$$J = -\frac{4e^2}{\hbar} Tr\left[\mathrm{Im}[\rho] \cdot \tilde{\tau}_D\right] . \tag{3-a}$$

Here $\tilde{\tau}_D \equiv \begin{pmatrix} 0 & \tau_D \\ 0 & 0 \end{pmatrix}$, and τ_D is the coupling matrix between two arbitrary portions of the defective region: $H_D \equiv \begin{pmatrix} h1 & \tau_D \\ \tau_D & h2 \end{pmatrix}$.

Computation of such a wealth of useful physical quantities requires only one non-trivial component – the self-energy matrix. The goal of this paper is to present the exact

non-recursive algorithm for construction of the self-energy matrixes $\Sigma_L[\varepsilon]$ and $\Sigma_R[\varepsilon]$. Extension to topologies with larger number of leads is straightforward.

III. ALGORITHM FOR SELF-ENERGY

Following each step number we indicate the number of the section, which contains the detailed description of the given step.

1. (Next article in this issue) For the given energy ε construct transfer matrix **T**. The size of **T** is even and equals $2P$. If τ is non-singular, $P = N$ and **T** has the well known 2×2 sub-block structure[11]

$$T = \begin{pmatrix} \tau^{-1} \cdot (\varepsilon I - h) & -\tau^{-1} \cdot \tau^{T} \\ I & 0 \end{pmatrix}, \tag{4}$$

where I is the identity matrix of the size N. The algorithm for the construction of **T** associated with singular τ is more complex and is presented in the next paper. The poor man's solution for the singular τ case is to make substitution $\tau \to \tau + \delta\tau$, where $\delta\tau$ is an arbitrary small non-singular matrix, and then apply Eq.(4). Usually this approach does not cause any noticeable change of the lead properties, e.g. its band structure, but may be not sufficient to obtain well-conditioned **T**.

Obtain the sets of $2P$ scalars $\{\Lambda_i\}$ and the corresponding $2P$ vectors $\{C_i\}$ of the length N. Λ_i and C_i satisfy the eigenproblem equation $H[\Lambda_i]\cdot C_i = \varepsilon C_i$, where

$$H[\Lambda] = \tau\Lambda + h + \tau^{T}\Lambda^{-1} . \tag{5}$$

If τ is non-singular, $\{\Lambda_i\}$ are simply the eigenvalues of matrix **T**, and $\{C_i\}$ are the vectors composed from the first N components of the corresponding eigenvectors.

2. (Sec. V) For every $\Lambda_\alpha \in \{\Lambda_i\}$ there is $\Lambda_\beta \in \{\Lambda_i\}$ such that $\Lambda_\alpha = \Lambda_\beta^{-1}$. Create the complimentary set $\{\tilde{C}_i\}$, which is the reordered set $\{C_i\}$. For $\alpha \in \{1, 2\ldots 2P\}$ the α^{th} entry of $\{\tilde{C}_i\}$ is vector $C_\beta \in \{C_i\}$ such that $\Lambda_\alpha = \Lambda_\beta^{-1}$. Normalize the sets $\{C_i\}$ and $\{\tilde{C}_i\}$:

$$C_\alpha \to \frac{C_\alpha}{\sqrt{\tilde{C}_\alpha^{\,T} \cdot C_\alpha}} , \qquad \tilde{C}_\alpha \to \frac{\tilde{C}_\alpha}{\sqrt{\tilde{C}_\alpha^{\,T} \cdot C_\alpha}}$$

3. (Sec. V). Compute the set $\{V_i\}$:

$$V_\alpha = i\ \tilde{C}_\alpha^{\ T} \cdot \left(\Lambda_\alpha\, \tau - \Lambda_\alpha^{-1}\, \tau^T \right) \cdot C_\alpha \quad , \qquad \alpha \in \{1, 2 \ldots 2\,P\} \tag{6}$$

4. (Sec. V). Compose the sets $\{Cs_i\}$, $\{Cs_i\}$, $\{Vs_i\}$, and $\{\Lambda s_i\}$ from the sets $\{C_i\}$, $\{\tilde{C}_i\}$, $\{V_i\}$ and $\{\Lambda_i\}$ respectively. Elements of $\{C_i\}$, $\{\tilde{C}_i\}$, $\{V_i\}$ and $\{\Lambda_i\}$ are selected respectively for the sets $\{Cs_i\}$, $\{Cs_i\}$, $\{Vs_i\}$, and $\{\Lambda s_i\}$ only if

$$|\Lambda_\alpha| < 1$$

or

$$|\Lambda_\alpha| = 1 \text{ and } V_\alpha > 0\ .$$

The size of the sets $\{Cs_i\}$, $\{Cs_i\}$, $\{Vs_i\}$, and $\{\Lambda s_i\}$ is P.

5. (Sec. V). Construct matrix $G_{1,0}$:

$$G_{1,0}[\varepsilon] = -i \sum_{\alpha=1}^{P} \frac{\Lambda s_\alpha}{Vs_\alpha} Cs_\alpha \cdot Cs_\alpha^{\ T} \tag{7}$$

Let CS and $\overline{CS}$ denote matrices, which columns are respectively the vectors of the sets $\{Cs_i\}$ and $\{Cs_i\}$. Let also VS and ΛS denote diagonal matrices with the elements on the main diagonal equal respectively the elements of the sets $\{Vs_i\}$, and $\{\Lambda s_i\}$. Then, Eq.(7) may me rewritten in a matrix form:

$$G_{1,0}[\varepsilon] = -i\ CS \cdot \Lambda S \cdot VS^{-1} \cdot \overline{CS}^{\,T} \tag{7-a}$$

The dimensions of $G_{1,0}$ are $N \times N$, while the dimensions of CS and $\overline{CS}$ are $N \times P$, and the dimensions of VS and ΛS are $P \times P$. If τ is nonsingular, $P = N$, and hence $G_{1,0}$ is also nonsingular. In τ is singular, $P < N$, and $G_{1,0}$ is singular as well.

6. (Sec. IV). Construct matrix $G_{0,0}$:

$$G_{0,0}\left[\varepsilon\right] = \left(\varepsilon \times I - h\right)^{-1} \cdot \left(I + \tau \cdot G_{1,0}\left[\varepsilon\right] + \tau^T \cdot G_{1,0}\left[\varepsilon\right]^T \right) \tag{8}$$

7. (Sec. IV). Construct self-energy matrices:

$$\Sigma_L\left[\varepsilon\right] = G_{0,0}\left[\varepsilon\right]^{-1} \cdot G_{1,0}\left[\varepsilon\right] \cdot \tau \tag{9-a}$$

$$\Sigma_R\left[\varepsilon\right] = G_{0,0}\left[\varepsilon\right]^{-1} \cdot G_{1,0}\left[\varepsilon\right]^T \cdot \tau^T \tag{9-b}$$

IV. SELF-ENERGY FROM GREEN'S FUNCTIONS OF INFINITE LEAD

Suppose that the imaginary plane divides the lead along the unit-cell boundary. Let H_L and H_R denote respectively the Hamiltonian matrix sub-blocks describing the portions of the lead to the left and to the right of the plane. Let H_{LR} denote the interaction between these two parts. By analogy the Green's matrix can be subdivided in the same fashion:

$$H = \begin{pmatrix} H_L & H_{LR} \\ H_{LR}^{\ T} & H_R \end{pmatrix} \qquad G = \begin{pmatrix} G_L & G_{LR} \\ G_{RL} & G_R \end{pmatrix}. \tag{10}$$

All sub-blocks are semi-infinite. The H_{LR} matrix has only a finite number of non-zero elements in the lower left corner due to the one-dimensional nature of the system and finite interaction radius between atomic orbitals. These non-zero elements constitute the matrix τ, which accounts for the coupling between the adjacent unit cells (cf. Fig. 1(b))

$$H_{LR} = \begin{pmatrix} \vdots & \vdots & \iddots \\ 0 & 0 & \cdots \\ \tau & 0 & \cdots \end{pmatrix}.$$

The identity $G\cdot((\varepsilon + i\,\eta) - H) = \mathbf{1}$ applied to matrices (10) results in four equations for the semi-infinite matrix sub-blocks. The equations for the left and the right upper sub-blocks respectively are

$$G_L \cdot \left((\varepsilon + i\eta)\ I - H_L \right) - I = G_{LR} \cdot H_{LR}^T, \tag{11-a}$$

$$G_{LR} \cdot \left((\varepsilon + i\eta)\ I - H_R \right) = G_L \cdot H_{LR}. \tag{11-b}$$

The expression in the parenthesis in Eq.(11-b) is the inverse Green's function for the *semi*-infinite right portion of the system $g^{(R)}$. Equation (11-b) can be transformed to

$$G_L^{-1} \cdot G_{LR} \cdot H_{LR}^{\ T} = H_{LR} \cdot g^{(R)} \cdot H_{LR}^{\ T}. \tag{11-c}$$

Though Eq.(11-c) involves semi-infinite matrixes, the dimension of the non-zero part of Eq.(11-c) is the same as the dimension of τ:

$$H_{LR} \cdot g^{(R)} \cdot H_{LR}^{\ T} =$$

$$\begin{pmatrix} \vdots & \vdots & \iddots \\ 0 & 0 & \cdots \\ \tau & 0 & \cdots \end{pmatrix} \cdot \begin{pmatrix} g_{0,0}^{(R)} & g_{0,1}^{(R)} & \cdots \\ g_{1,0}^{(R)} & g_{1,1}^{(R)} & \cdots \\ \vdots & \vdots & \ddots \end{pmatrix} \cdot \begin{pmatrix} \cdots & 0 & \tau^T \\ \cdots & 0 & 0 \\ \iddots & \vdots & \vdots \end{pmatrix} = \begin{pmatrix} \ddots & \vdots & \vdots \\ \cdots & 0 & 0 \\ \cdots & 0 & \tau \cdot g_{0,0}^{(R)} \cdot \tau^T \end{pmatrix}.$$

Here $g^{(R)}{}_{i,j}$ are the sub-blocks of $g^{(R)}$, which have the same dimensions as τ. The product $\tau \cdot g^{(R)}{}_{0,0} \cdot \tau^T$ appears to be the self-energy matrix, which accounts for the contact to the semi-infinite right portion of the lead. To show that this is indeed the case we express G_{LR} from Eq.(11-b) and substitute it into Eq.(11-a)

$$G_L^{-1} = (\varepsilon + i\eta)\ I - \left(H_L + H_{LR} \cdot g^{(R)} \cdot H_{LR}^T\right).$$

By definition, the quantity Σ_R, which should be added to H_L, so that

$$G_L^{-1} = (\varepsilon + i\eta)\ I - \left(H_L + \Sigma_R\right)$$

is the self-energy accounting for the contact with the right portion of the lead. The non-zero part of Σ_R is

$$\Sigma_R = \tau \cdot g_{0,0}^{(R)} \cdot \tau^T = \tau \cdot \left((\varepsilon + i\eta)\ I - h - \Sigma_R\right)^{-1} \cdot \tau^T . \qquad (12\text{-a})$$

The latter equality constitutes the well known recursion relation for the self-energy, which can be proven as follows. The upper-left corner sub-block $g^{(R)}{}_{0,0}$ of the semi-infinite Green's function matrix $g^{(R)}$ corresponds to the rightmost unit cell of the semi-infinite lead. If this unit cell were not connected to the semi-infinite extension through its right boundary, the expression for $g^{(R)}{}_{0,0}$ would be $g^{(R)}{}_{0,0} = ((\varepsilon + i\,\eta) - h)^{-1}$. By the definition, the connection to the semi-infinite lead through the right boundary amounts to the addition to the Hamiltonian, which is h in that case, the self-energy matrix Σ_R, i.e. $g^{(R)}{}_{0,0} = ((\varepsilon + i\,\eta) - h - \Sigma_R)^{-1}$. The analogous expression for Σ_L is

$$\Sigma_L = \tau^T \cdot g_{0,0}^{(L)} \cdot \tau = \tau^T \cdot \left((\varepsilon + i\eta)\ I - h - \Sigma_L\right)^{-1} \cdot \tau . \qquad (12\text{-b})$$

To obtain a computationally tractable non-recursive expression for Σ_R we need to rewrite Eq.(11-c) in the sub-block form:

$$G_{LR} \cdot H_{LR}{}^T = G_L \cdot \left(H_{LR} \cdot g^{(R)} \cdot H_{LR}{}^T\right)$$

$$\Downarrow$$

$$\begin{pmatrix} \vdots & \vdots & \iddots \\ X & X & \cdots \\ G_{0,1} & X & \cdots \end{pmatrix} \cdot \begin{pmatrix} \cdots & 0 & \tau^T \\ \cdots & 0 & 0 \\ \iddots & \vdots & \vdots \end{pmatrix} = \begin{pmatrix} \ddots & \vdots & \vdots \\ \cdots & X & X \\ \cdots & X & G_{0,0} \end{pmatrix} \cdot \begin{pmatrix} \ddots & \vdots & \vdots \\ \cdots & 0 & 0 \\ \cdots & 0 & \Sigma_R \end{pmatrix}$$

$$\Downarrow$$

$$\begin{pmatrix} \ddots & \vdots & \vdots \\ \cdots & 0 & X \\ \cdots & 0 & G_{0,1}\cdot\tau^T \end{pmatrix} = \begin{pmatrix} \ddots & \vdots & \vdots \\ \cdots & 0 & X \\ \cdots & 0 & G_{0,0}\cdot\Sigma_R \end{pmatrix},$$

where X marks non-zero sub-blocks. Equating low-right corner sub-blocks in the last equation, and using the symmetry of the Green's function matrix, i.e. $G_{1,0}{}^{\mathrm{T}} = G_{0,1}$, we obtain the compact analogues of Eq.(11-c):

$$\begin{aligned} \Sigma_R &= G_{0,0}{}^{-1}\, G_{1,0}^T\, \tau^T \quad , \\ \Sigma_L &= G_{0,0}{}^{-1}\, G_{1,0}\, \tau \quad . \end{aligned} \tag{11-d}$$

Here $G_{0,0}$, $G_{1,0}$, and $G_{0,1}$ are the Green's function sub-blocks of the same size as τ. They are respectively diagonal, below diagonal, and above diagonal sub-blocks of the infinite Green's matrix associated with the infinite translationally symmetric lead.

For the reasons that will become apparent in the next section it is convenient to express $G_{0,0}$ through $G_{1,0}$ and to use $G_{1,0}$ as the only Green's function sub-block involved in the self-energy computation. This can be done by using the identity $((\varepsilon + i\,\eta) - H)\cdot G = \mathbf{1}$ for the infinite lead

$$\begin{pmatrix} \ddots & \vdots & \vdots & \vdots & \iddots \\ \cdots & I\times\varepsilon - h & -\tau & 0 & \cdots \\ \cdots & -\tau^T & I\times\varepsilon - h & -\tau & \cdots \\ \cdots & 0 & -\tau^T & I\times\varepsilon - h & \cdots \\ \iddots & \vdots & \vdots & \vdots & \ddots \end{pmatrix} \cdot \begin{pmatrix} \ddots & \vdots & \vdots & \vdots & \iddots \\ \cdots & G_{0,0} & G_{1,0}^T & G_{2,0}^T & \cdots \\ \cdots & G_{1,0} & G_{0,0} & G_{1,0}^T & \cdots \\ \cdots & G_{2,0}^T & G_{1,0} & G_{0,0} & \cdots \\ \iddots & \vdots & \vdots & \vdots & \ddots \end{pmatrix} = 1 \ . \tag{13}$$

Multiplying central row by the central column we obtain the expression for $G_{0,0}$

$$G_{0,0} = \left(I\times\varepsilon - h\right)^{-1}\cdot\left(I + \tau\cdot G_{1,0} + \tau^T\cdot G_{1,0}^T\right) \ . \tag{14}$$

V. EXPRESSION FOR $G_{1,0}$

$G_{1,0}$ is the only sub-block of the Green's function matrix of an infinite periodic lead, which is required for self-energy computation. The Green's function of the infinite lead is the infinite size matrix formally defined as $(I\,(\varepsilon + i\,\eta) - H)^{-1}$, where H is the infinite Hamiltonian matrix. The usual strategy for the computation of the Green's function matrix elements is to switch from local to plane-wave basis set. As a result the infinite matrix $(I\,(\varepsilon + i\,\eta) - H)$ transforms to the finite size invertible matrix $(I\,(\varepsilon + i\,\eta) - H[K])$. Af-

ter that one needs to transform $(I\,(\varepsilon + i\,\eta) - H[K])^{-1}$ back to the atomic orbital basis. This reverse transformation involves integration over plane-wave variable K. The numerical integration over K is imprecise and computationally expensive because $(I\,(\varepsilon + i\,\eta) - H[K])^{-1}$ has van-Hove singularities along the real K-axis. However, there is the elegant way to substitute the real-axis integration by the contour integration in the complex K-plane. We choose the contour for which the contour contribution to the integral vanishes, and the integral equals to the sum of the residues. We start deriving the expression for $G_{1,0}$ with the integral expression for the Green's function. The plane-wave basis functions are chosen as

$$\left|K,\alpha\right\rangle = A\sum_{n=-\infty}^{\infty}\left|n,\alpha\right\rangle Exp\left[i\,K\,n\right]\ ,\quad a \in \{1,\,N\}. \tag{15}$$

Here $|n,\,\alpha\rangle$ is α^{th} atomic orbital in the n^{th} unit cell, and A is the normalization factor. In this basis the tri-block-diagonal Hamiltonian (Fig. 1(b)) has the form

$$\begin{aligned}&\left\langle K,\alpha\middle|H\middle|K,\beta\right\rangle \equiv H\left[K\right]_{\alpha,\beta} = \left(\tau^{T}\,Exp\left[-i\,K\right] + h + \tau\,Exp\left[i\,K\right]\right)_{\alpha,\beta}\\ &\left\langle K_1,\alpha\middle|H\middle|K_2,\beta\right\rangle = 0 \qquad if\quad K_1 \neq K_2\ .\end{aligned} \tag{16}$$

In some cases it is more convenient to operate with variable $\Lambda = Exp[i\,K]$. Mapping $K \leftrightarrow \Lambda$ is reversible if we agree that $-\pi \le \mathrm{Re}[K] \le \pi$. Hence the alternative form for Eq.(16) is

$$H\left[\Lambda\right]_{\alpha,\beta} = \left(\tau^{T}\,\Lambda^{-1} + h + \tau\,\Lambda\right)_{\alpha,\beta} \tag{16-a}$$

Next we invert $(I\,(\varepsilon + i\,\eta) - H[K])$ and return back to the atomic orbital basis. The expression for the Green's function matrix element is

$$\left\langle m,\alpha\middle|G\middle|n,\beta\right\rangle = \int_{-\pi}^{\pi}\frac{Exp\left[i\,K\left(m-n\right)\right]}{2\pi}\left\{\left(I\,\left(\varepsilon + i\,\eta\right) - H\left[K\right]\right)^{-1}\right\}_{\alpha,\beta}dK\ . \tag{17}$$

The alternative to integration from $-\pi$ to π along the real axis is the integration over the contour composed of three parts (Fig. 3): from $-\pi$ to $-\pi + i\infty$, from $-\pi + i\infty$ to $\pi + i\infty$, and from $\pi + i\infty$ to π. The integrals over the first and the third parts of the contour cancel because $H[-\pi + i\,\mathrm{Im}[K]] = H[\pi + i\,\mathrm{Im}[K]]$. To investigate the behavior of the integral over infinitely remote segment $[\pi + i\,\infty,\ \pi + i\,\infty]$ it is convenient to view the integrand in Eq.(17) as

$$\frac{Exp\left[iK\left(m-n\right)\right]}{2\pi}\left\{\left(I\left(\varepsilon+i\,\eta\right)-H\left[K\right]\right)^{-1}\right\}_{\alpha,\beta}=e^{iK}\,\frac{\left(-1\right)^{\alpha+\beta}M_{\alpha,\beta}}{Det\left[I\left(\varepsilon+i\,\eta\right)-H\left[K\right]\right]}\ . \qquad (18)$$

Here $M_{\alpha,\beta}$ is minor for the corresponding element of matrix ($I\,\varepsilon - H[K]$). As it follows from Eq.(16), the right hand side of Eq.(18) can be viewed as

$$e^{iK}\times\frac{B_0+\sum_{n=1}^{R}\left(B_n^{-}\,e^{-iKn}+B_n^{+}\,e^{+iKn}\right)}{A_0+\sum_{n=1}^{S}\left(A_n^{-}\,e^{-iKn}+A_n^{+}\,e^{+iKn}\right)}\xrightarrow{\mathrm{Im}[K]\to+\infty}e^{iK}\times\frac{B_0+\sum_{n=1}^{R}B_n^{-}\,e^{-iKn}}{A_0+\sum_{n=1}^{S}A_n^{-}\,e^{-iKn}}\ , \qquad (18\text{-a})$$

where A_i and B_i are independent of K. If τ is non-singular, $S = N$, $R = N - 1$, and the ratio in the right hand side of Eq.(18-a) tends to 0 when $\mathrm{Im}[K] \to \infty$. In the case when τ is singular, the largest possible $R = S$, and hence

$$Max\left[\underset{\mathrm{Im}[K]\to+\infty}{Lim}\left[\frac{B_0+\sum_{n=1}^{R}B_n^{-}\,e^{-iKn}}{A_0+\sum_{n=1}^{S}A_n^{-}\,e^{-iKn}}\right]\right]=Const\ . \qquad (18\text{-b})$$

However, the exponential factor in front of this ratio makes it 0 for $\mathrm{Im}[K] \to +\infty$. Therefore the contribution from the infinitely remote part of the integration contour is 0 regardless the type of τ. This is true only for the elements of the Green's function $\langle\alpha, m|G|n, \beta\rangle$ belonging to the sub-blocks lying below the main diagonal, i.e. for $m > n$, because only in this case the exponential factor in Eq.(17) tends to 0 as $\mathrm{Im}[K] \to +\infty$. For that reason we do not apply contour integration to evaluation of $G_{0,0}$, but rather compute it through $G_{1,0}$ using Eq.(14).

The only contribution to the contour integral is from the poles (Fig. 4), thus Eq.(17) transforms to

$$\left\langle m,\alpha\middle|G\middle|n,\beta\right\rangle=i\sum_{s}Exp\left[iK_s\left(m-n\right)\right]\,res\left[\left\{\left(I\left(\varepsilon+i\,\eta\right)-H\left[K_s\right]\right)^{-1}\right\}_{\alpha,\beta}\right]. \qquad (19)$$

Here the summation is performed over all poles K_s inside the contour, i.e. $-\pi \le \mathrm{Re}[K_s] < \pi$ and $\mathrm{Im}[K_s] \ge 0$. $(I\,(\varepsilon + i\,\eta) - H[K_s])^{-1}$ can be expressed as

$$\left(I\left(\varepsilon+i\,\eta\right)-H\left[K_s\right]\right)^{-1}=\sum_{n}\frac{C_n\left[K\right]\cdot\tilde{C}_n\left[K\right]^{T}}{\left(\varepsilon+i\,\eta\right)-\varepsilon_n}\ ,\ \text{where} \qquad (20)$$

$C_n[K]$ and $\varepsilon_n[K]$ are the eigenvector and corresponding eigenvalue of $H[K]$, and

$$H[K]^T \cdot \tilde{C}_n[K] = \varepsilon_n \tilde{C}_n[K] \quad \text{or} \quad \tilde{C}_n[K]^T \cdot H[K] = \varepsilon_n \tilde{C}_n[K]^T . \tag{20-a}$$

From Eq.(20-a) it follows that $\tilde{C}_n[K]$ and $C_n[K]$ are orthogonal, and we assume that these vectors are normalized

$$\tilde{C}_i[K]^T \cdot C_j[K] = \delta_{i,j} \quad \text{and} \quad \sum_i \tilde{C}_i[K] \cdot C_i[K]^T = I . \tag{20-b}$$

At the pole K_s one of the eigenvalues of $H[K_s]$ is $\varepsilon_r = (\varepsilon + i\,\eta)$. In the vicinity of K_s only one term in the sum (20) is proportional to $(K - K_s)^{-1}$:

$$\frac{C_r[K_s] \cdot \tilde{C}_r[K_s]^T}{-\left.\frac{\partial \varepsilon_r[K]}{\partial K}\right|_{K=K_S} (K - K_s)} . \tag{21}$$

Thus, Eq.(19) can be rewritten as

$$\langle m, \alpha | G | n, \beta \rangle = i \sum_s Exp\left[i K_s (m-n) \right] \frac{\left(C_r[K_s] \cdot \tilde{C}_r[K_s]^T \right)_{\alpha,\beta}}{-\left.\frac{\partial \varepsilon_r[K]}{\partial K}\right|_{K=K_S}} . \tag{22}$$

The derivative in the denominator of Eq.(22) is computed in a usual manner: we multiply the Schrödinger equation by $\tilde{C}_r[k]$ and differentiate it over K

$$\frac{\partial \left(\tilde{C}_r[K]^T \cdot H[K] \cdot C_r[K] \right)}{\partial K} = \frac{\partial \left(\varepsilon_r[K]\, \tilde{C}_r[K]^T \cdot C_r[K] \right)}{\partial K} . \tag{23}$$

Using Eqs.(20-a) and (20-b) we obtain

$$\frac{\partial \varepsilon_r[K]}{\partial K} = \tilde{C}_r[K]^T \cdot \left(\frac{\partial H[K]}{\partial K} \right) \cdot C_r[K] , \tag{24}$$

where $\partial H[K]/\partial K$ is computed using Eq.(16). Assembling together Eqs.(24), (22), and (16), and keeping in mind that for the first sub-diagonal block $m - n = 1$, we obtain the expression for G_{10}

$$G_{1,0}[\varepsilon] = -\sum_s \frac{Exp[i K_s]\, C_r[K_s] \cdot \tilde{C}_r[K_s]^T}{\tilde{C}_r[K_s]^T \cdot \left(\tau\, Exp[i K_s] - \tau^T Exp[-i K_s] \right) \cdot C_r[K_s]} , \tag{25}$$

which is identical to Eq.(7). The poles positions, i.e. the values of K_s, and corresponding vectors $C_r[K]$ and $\tilde{C}_r[K]$ are obtained using transfer matrix technique. Since $H[-K] = H[K]^T$, for every pole K_s such that $H[K_s] \cdot C_r[K_s] = \varepsilon_r C_r[K_s]$ there exists symmetric pole

$-K_s$ such that $H[-K_s]\cdot C_r\left[-K_s\right] = H[K_s]^T\cdot \tilde{C}_r\left[K_s\right] = \varepsilon_r\, \tilde{C}_r\left[K_s\right]$. This explains the correspondence between the sets $\{C_n\}$ and $\{\tilde{C}_n\}$, and hence the procedure described in step 2 of section III.

If $\mathrm{Im}[K_s] \neq 0$, only K_s lying inside the integration contour, i.e. with $|\Lambda_s| < 1$, should be included in the sum (25). For real ε some poles may lie on the real axis: $\varepsilon_r[K_s] = \varepsilon$, $\mathrm{Im}[K_s] = 0$. In this case one needs to use first order expansion of $\varepsilon_r[K]$ in the vicinity of K_s to determine which poles lie inside the contour, at the distance δK_s infinitesimally above real axis. The pole condition is formulated as $\varepsilon_r[K_s + i\,\delta K_s] = \varepsilon + i\,\eta$, which in the first order approximation means $i\,\partial\varepsilon_r[K]/\partial K = i\,\eta$. Since $\eta > 0$, the selection condition for the real axis poles is

$$\left.\frac{\partial\,\varepsilon_r\left[K\right]}{\partial K}\right|_{K=K_s} > 0\,.$$

That completes the proof of the algorithm presented in section III.

VI. EXTENSION FOR MULTI-BLOCK-BAND HAMILTONIAN

If the interaction range between a unit cell and neighbor cells in a 1-D translationally periodic lead is $W > 1$, the localized basis Hamiltonian matrix has $2W+1$ block-bands. In the extended basis set given by Eq.(15) $H[k]$ has the form:

$$H\left[k\right] = h^{(0)} + \sum_{n=1}^{R}\left(h^{(n)T}\,Exp\left[-i\,k\,n\right] + h^{(n)}\,Exp\left[i\,k\,n\right]\right)\,, \tag{16-b}$$

$$H\left[\lambda\right] = h^{(0)} + \sum_{n=1}^{R}\left(h^{(n)T}\,\lambda^{-n} + h^{(n)}\,\lambda^{n}\right), \quad \lambda \equiv Exp\left[i\,k\right]\,, \tag{16-c}$$

where $h^{(n)}$ is the sub-block located n blocks above the main diagonal. For the example depicted in Fig. 1(a) $W = 2$, and $h^{(0)} = h$, $h^{(1)} = \tau$, and $h^{(2)} = \chi$. The general case algorithm for the computation of $\{\lambda_i\}$ and $\{c_i\}$, such that $H[\lambda_i]\cdot c_i = \varepsilon\, c_i$, and $H[\lambda]$ is given by Eq.(16-c), is provided in the next paper. If $\{\lambda_i\}$ and $\{c_i\}$ are known, one can choose two different ways to compute G_{10}. The simplest one is to obtain $\{\Lambda_i\}$ and $\{C_i\}$, which are the solutions of the corresponding tri-block-diagonal Eq.(16-a). As it is shown in the next paper, $\Lambda_i = \lambda_i^{\,W}$ and vectors C_i are obtained by joining vectors $c_i\,\lambda_i^{\,n}$: $C_i = \{c_i,\ c_i\,\lambda_i,\ c_i\,\lambda_i^{\,2},\ \ldots,\ c_i\,\lambda_i^{\,W-1}\}$. After that, the algorithm from section III is applied without changes.

The alternative is to assemble G_{10} from the sub-blocks of the same size as $h^{(n)}$. For example, if $W = 3$

$$G_{1,0} = \begin{pmatrix} g_{3,0} & g_{2,0} & g_{1,0} \\ g_{4,0} & g_{3,0} & g_{2,0} \\ g_{5,0} & g_{4,0} & g_{3,0} \end{pmatrix},$$

where sub-blocks $g_{m,0}$ are evaluated using the general expression for $\langle \alpha,\ m \mid G \mid n,\ \beta \rangle$ (Eq.(22)):

$$g_{m,0}[\varepsilon] = -\sum_s \frac{\lambda_s^m c_s \cdot \tilde{c}_s^{\,T}}{\tilde{c}_s^{\,T} \cdot \left(\sum_{n=1}^{W} n \left(h^{(n)} \lambda_s^n - h^{(n)T} \lambda_s^{-n} \right) \right) \cdot c_s} \ . \qquad \text{(22-a)}$$

This method is slightly faster because the denominator in Eq.(22-a) is the same for all $g_{m,0}$, and needs to be calculated only once. In other respects the multi-band case is treated in the same fashion as the tri-block-diagonal.

VII. EXTENSION FOR SCREW SYMMETRY

We start the consideration of the screw symmetry with the tri-block-diagonal case. Now sub-block matrixes h and τ are different for different cells, but related to each other through the rotation around the screw axis (Fig. 5). We pick up the cell with index 0, and assume that its Hamiltonian sub-block is h, while the coupling matrix between the cells with indexes 0 and 1 is τ. Other sub-blocks of the infinite Hamiltonian describing 1-D lead are related to h and τ as follows from Eq.(26)

$$H = \begin{pmatrix} \ddots & \vdots & \vdots & \vdots & \vdots & \vdots & \iddots \\ \cdots & R^{-2} \cdot h \cdot R^2 & R^{-2} \cdot \tau \cdot R^2 & 0 & 0 & 0 & \cdots \\ \cdots & R^{-2} \cdot \tau^T \cdot R^2 & R^{-1} \cdot h \cdot R & R^{-1} \cdot \tau \cdot R & 0 & 0 & \cdots \\ \cdots & 0 & R^{-1} \cdot \tau^T \cdot R & h & \tau & 0 & \cdots \\ \cdots & 0 & 0 & \tau^T & R \cdot h \cdot R^{-1} & R \cdot \tau \cdot R^{-1} & \cdots \\ \cdots & 0 & 0 & 0 & R \cdot \tau^T \cdot R^{-1} & R^2 \cdot h \cdot R^{-2} & \cdots \\ \iddots & \vdots & \vdots & \vdots & \vdots & \vdots & \ddots \end{pmatrix} . \qquad (26)$$

Here R is the orbital rotation matrix, which is convenient to define through the Bloch theorem for 1-D systems with screw symmetry. If $C_i^{(0)}$ is the portion of the wave-vector corresponding to the unit cell with index 0, the wave-vector for the entire system is:

$$C_i^{\infty} \equiv \begin{pmatrix} \vdots \\ R^{-2} \cdot C_i^{(0)} \times \Lambda_i^{-2} \\ R^{-1} \cdot C_i^{(0)} \times \Lambda_i^{-1} \\ C_i^{(0)} \\ R \cdot C_i^{(0)} \times \Lambda_i \\ R^{2} \cdot C_i^{(0)} \times \Lambda_i^{2} \\ \vdots \end{pmatrix} . \qquad (27)$$

The analog of Eq.(15) for the system with a screw symmetry is

$$\left|K,\alpha\right\rangle = A\sum_{n=-\infty}^{\infty} R^n \left|n,\alpha\right\rangle Exp\left[iKn\right] , \quad a \in \{1, N\}, \qquad (15\text{-a})$$

and hence the analog of Eq.(16-a) is

$$H\left[\Lambda\right] = \left(\left(\tau \cdot R\right)^{\mathrm{T}} \Lambda^{-1} + h + \left(\tau \cdot R\right)\Lambda\right). \qquad (16\text{-d})$$

Here we used unitarity of R: $R^{-1} = R^T$. Thus, the only difference between screw and translational symmetries is the substitution of τ by $\tau \cdot R$. The algorithm presented in section III can be used without changes provided $\tau \to \tau \cdot R$. Now, however, the self-energies are not translationally invariant. That means the algorithm in section III generates Σ_L, which represents the effect of the contact with the left-going lead only for the boundary between unit cells with indexes –1 and 0. Similarly Σ_R represents the effect of the contact with the right-going lead only for the boundary between unit cells with indexes 0 and 1. The self-energy, which accounts for the contact with the left-going lead at the boundary between unit cells $n - 1$ and n is $\Sigma_L^{(n)} = R^n \cdot \Sigma_L^{(0)} \cdot R^n$. The self-energy, which accounts for the contact with the right-going lead at the boundary between unit cells n and $n + 1$ is $\Sigma_R^{(n)} = R^n \cdot \Sigma_R^{(0)} \cdot R^n$ (Fig. 6). This transformation rule is equally applicable to the multi-block-band Hamiltonian. Analogously to the multi-block-band case for the translationally symmetric system, $\Lambda_i = \lambda_i^W$ and vectors C_i are obtained by joining vectors $R^n \cdot c_i \lambda_i^n$: $C_i = \{c_i, R^1 \cdot c_i \lambda_i, R^2 \cdot c_i \lambda_i^2, \ldots, R^{W-1} \cdot c_i \lambda_i^{W-1}\}$. After that, the algorithm from section III is applied provided $\tau \to \tau \cdot R$.

VIII. LOCALIZATION LENGTH IN RANDOMLY DISTORTED NANO-TUBES

In this section we derive the expression for the current deviation from its ideal ballistic value for a randomly distorted nano-tube. Derivation is based on Eq.(19), the general expression for $\langle \alpha, m|G|n, \beta\rangle$. Knowing the dependence of the current deviation on the length of the distorted region we evaluate the localization length.

Based on the Eq.(2-a) and the Landauer's equation (3-a), the contribution to the total current from the electrons with energy ε is

$$I[\varepsilon] = -\frac{2e^2}{h}\ 4\ Tr\left[\mathrm{Im}\left[G_{A+B}[\varepsilon] \cdot \mathrm{Im}\left[\tilde{\Sigma}_R[\varepsilon] \right] \cdot G^*_{A+B}[\varepsilon] \right] \cdot \begin{pmatrix} 0 & h_{AB} \\ 0 & 0 \end{pmatrix} \right]. \qquad \text{(3-b)}$$

Here G_{A+B} is the Green's function of an arbitrary portion of the lead, which is sub-divided in parts A and B, and h_{AB} is the Hamiltonian coupling matrix between these parts. If we choose A and B to be the adjacent unit cells located to the right from the distorted region, (Fig. 7), $h_{AB} = \tau$, and matrix $\tilde{\Sigma}_R$ corresponds to the ideal right-going lead. The size of G_{A+B} and $\tilde{\Sigma}_R$ is twice the size of τ. To acknowledge that we use $G_{2\times2}$ and $\Sigma RIdeal_{2\times2}$ instead of G_{A+B} and $\tilde{\Sigma}_R$. Since $G_{2\times2}$ corresponds to the perfect undistorted cells, its deviation from the Green's function of the perfect wire, which we denote as $\Delta G_{2\times2} = GIdeal_{2\times2} - G_{2\times2}$, is stipulated solely by $\Delta\Sigma_{2\times2} \equiv \Sigma LIdeal_{2\times2} - \Sigma L_{2\times2}$. The difference between $I[\varepsilon]$ and the current in the perfect lead can be expressed as [16]

$$\Delta I[\varepsilon] \equiv I_{Ideal}[\varepsilon] - I[\varepsilon] = -\frac{4e^2}{\pi\hbar}\mathrm{Tr}\left[\mathrm{Im}\left[\Delta G_{2\times2} \cdot \mathrm{Im}\left[\Sigma RIdeal_{2\times2} \right] \cdot \Delta G^*_{2\times2} \right] \cdot \tilde{\tau} \right]. \qquad (28)$$

Equation (28) is exact for any magnitude of $\Delta G_{2\times2}$. The first order expansion of $\Delta G_{2\times2}$ with respect to $\Delta\Sigma_{2\times2}$ allows to transform Eq.(28) as

$$\Delta I[\varepsilon] = -\frac{4e^2}{\pi\hbar}\mathrm{Tr}\Big[\mathrm{Im}\big[GIdeal_{2\times2} \cdot \Delta\Sigma L_{2\times2} \cdot GIdeal_{2\times2} \cdot \mathrm{Im}\big[\Sigma RIdeal_{2\times2} \big] \cdot GIdeal^*_{2\times2} \cdot \Delta\Sigma L^*_{2\times2} \cdot GIdeal^*_{2\times2} \cdot \tilde{\tau} \big] \Big]. \qquad (29)$$

Next we use Eq.(12-b) to expand $\Delta\Sigma L_{2\times2}$ with respect to the distortion $\delta H'$:

$$\Delta\Sigma L' \approx \tau'^T \cdot \left((\varepsilon + i\eta)\ I - H'_{(0)} - \Sigma L'_{(0)} \right)^{-1} \cdot \delta H' \cdot \left((\varepsilon + i\eta)\ I - H'_{(0)} - \Sigma L'_{(0)} \right)^{-1} \cdot \tau' \quad , \qquad (30)$$

where subscript (0) marks the matrixes associated with the ideal lead. Combining Eqs.(9-a) and (12-b) we can write the two first terms of Eq.(30) as

$$\tau'^{T}\cdot\left(\left(\varepsilon+i\eta\right)\,I-H'_{(0)}-\Sigma'_{(0)}\right)^{-1}=G'^{-1}_{0,0}\cdot G'_{1,0}\ . \tag{31}$$

If Eqs.(30)-(31) refer to the entire region between the points 1 and 2 in Fig. 7, the size of matrixes in Eq.(30)-(31) is $N\times(N_{\mathrm{D}}+N_I)$. Matrix τ'^{T} contains only one non-zero sub-block τ^{T} located in the upper-right corner, which means that only the upper sub-block row in the product $G'^{-1}_{0,0}\cdot G'_{1,0}$ differs from zero

$$G'^{-1}_{0,0}\cdot G'_{1,0}=\begin{pmatrix}\left(\varepsilon+i\eta\right)\,I-h-\Sigma_L^{(0)} & -\tau & 0 & \cdots\\ \vdots & \ddots & \cdots & \cdots\\ \vdots & \vdots & \ddots & \cdots\\ \vdots & \vdots & \vdots & \ddots\end{pmatrix}\cdot\begin{pmatrix}\cdots & \cdots & G_{N_D+N_I-j+1,0} & \cdots\\ \cdots & \cdots & G_{N_D+N_I-j+2,0} & \cdots\\ \vdots & \vdots & \vdots & \vdots\\ \vdots & \vdots & \vdots & \vdots\end{pmatrix}\cdot \tag{32}$$

In Eq.(32) we have explicitly shown the sub-blocks in j^{th} column of matrix $G'_{1,0}$. In the following we suppose the diagonal form for the distortion $\delta H'$. If the sub-block of $\delta H'$ corresponding to j^{th} unit cell is denoted as δh_j, Eqs.(30)-(32) can be combined as

$$\begin{aligned}\Delta\Sigma_L=\sum_{j=1}^{N_D}\Big(\Big(\left(\varepsilon+i\eta\right)\,I-h-\Sigma Ideal_L\Big)\cdot G_{N_D+N_I-j+1,0}-\tau\cdot G_{N_D+N_I-j+2,0}\Big)\cdot\\ \delta h_j\cdot\Big(G^{T}_{N_D+N_I-j+1,0}\cdot\Big(\left(\varepsilon+i\eta\right)\,I-h-\Sigma Ideal_L\Big)-G^{T}_{N_D+N_I-j+2,0}\cdot\tau^{T}\Big)\quad ,\end{aligned} \tag{33}$$

where $\Sigma Ideal_L$ is the self-energy at point 1 corresponding to the perfect left-going lead (Eq.(9-b)). Further transformation of Eq.(33) utilizes the analog of Eq.(7-a), which follows from Eq.(19)

$$G_{n,0}[\varepsilon]=-i\ CS\cdot\Lambda S^{n}\cdot VS^{-1}\cdot CS^{T},\quad n>0\ . \tag{7-b}$$

If we assume that N_I is sufficiently large, the diagonal matrix $\Lambda S^{N_D+N_I-j+1}$ has non-zero entries only for $|\Lambda s_\alpha|$ = 1, all other elements vanish. That means the product $\Lambda S^{N_D+N_I-j+1}\cdot CS^{T}$ contains only those vectors, which correspond to propagating waves, and hence $\Lambda S^{N_D+N_I-j+1}\cdot CS^{T}=\Lambda S^{N_D+N_I-j+1}\cdot CS^{\dagger}$. Thus we can write Eq.(33) as

$$\Delta\Sigma_L=f\cdot A\cdot f^{T},\ \text{where} \tag{34}$$

$$A=\sum_{j=1}^{N_D}\Big(\Lambda S^{N_D+N_I-j+1}\cdot VS^{-1}\cdot CS^{\dagger}\cdot\delta h_j\cdot C^{*}\cdot VS^{-1}\cdot\Lambda S^{N_D+N_I-j+1}\Big)$$

$$f = \left((\varepsilon + i\eta)\ I - h - \Sigma Ideal_L \right) \cdot CS - \tau \cdot CS \cdot \Lambda S$$

It is convenient to assume that all $|\Lambda s_\alpha| = 1$ are assembled in the upper part of ΛS. Since $A_{\alpha,\beta} \neq 0$ only if both α and β correspond to the states, which can propagate in the ideal lead, all non-zero elements of A are located in the upper-left corner sub-block. Substituting Eq.(34) into Eq.(29) we obtain

$$\Delta I\left[\varepsilon\right] = \frac{4e^2}{\pi\hbar} \sum_{\alpha,\beta,\gamma}^{N} \mathrm{Im}\left[A_{\alpha,\beta}\ J_{\beta,\beta}\ A^*_{\beta,\gamma}\ F_{\alpha,\gamma} \right], \tag{35}$$

where $F = f^T \cdot G_{1,0}{}^T \cdot \tau^T \cdot G_{0,0}{}^* \cdot f^*$ appears to be the diagonal matrix, and $J = f^\dagger \cdot G_{1,0}{}^\dagger \cdot \mathrm{Im}[\Sigma Ideal_R]\ \cdot G_{1,0} \cdot f$. We perform the statistical averaging of $\Delta I\,[\varepsilon]$ assuming the same dispersion σ for all elements of δh_j as well as no correlation between them. We also suppose that the distorted region is sufficiently long, so that $N_D >> 1$. The latter assumption means that we can neglect those terms in the sum (35), which contain "uncompensated" $\Lambda s_n{}^j$. Therefore the summation over cell index j in Eq.(34) transforms to the factor N_D in front of the sum (35). The average of Eq.(35) is

$$\Delta I\left[\varepsilon\right] = \frac{4e^2}{\pi\hbar} N_D\, \sigma^2\, \mathrm{Im}\left[\ \vec{J} \cdot B \cdot \vec{F}\ \right]. \tag{36}$$

Here vectors $\vec{J}$ and $\vec{F}$ contain the diagonal elements of matrixes J and F, and elements of matrix B are

$$B_{\alpha,\beta} = |Vs_\alpha|^{-2}\ \ |Vs_\beta|^{-2}\ Cs_\alpha^{(Sq)} \cdot Cs_\beta^{(Sq)} \quad \text{if } |\Lambda s_\alpha| = 1 \text{ and } |\Lambda s_\beta| = 1, \tag{37}$$

and 0 otherwise. Vector $Cs_n{}^{(Sq)}$ contains absolute squared components of the corresponding vector Cs_n. $\vec{J}$, $\vec{F}$, and $Cs_\alpha{}^{(Sq)} \cdot Cs_\beta{}^{(Sq)}$ are smooth functions of ε and hardly participate in the energy dependence of ΔI. On the contrary $Vs_\alpha{}^{-1}$ strongly depend on ε showing van-Hove singularities at the band edges. Roughly speaking $\Delta I\,[\varepsilon]$ is proportional to the squared number of open channels and to the density of states in the fourth power.

We apply Eqs.(36)-(37) to randomly distorted (11,10) nano-tube. We use π-orbital tight-binding in the nearest neighbor approximation with single hopping value $V_{\pi\pi}$ = -2.7 eV. Diagonal elements of δh_j are random numbers in the interval [-0.05 eV, +0.05 eV], which means that $\sigma^2 = 0.05^2/3$. The number of defective cells N_D is 10^3. Smooth line in Fig. 8 corresponds to $\Delta I\,[\varepsilon]$ computed using Eqs.(36)-(37). The rugged line is $\Delta I[\varepsilon]$ computed for the fixed set of random matrixes δh_j, $j = \{1,\ldots,10^3\}$. The most noti-

ceable feature in Fig 8 is the very low current deviation from its ideal value at the first conduction step. This effect is indeed descried by Eqs.(36)-(37): firstly, there are only four non-zero terms in quadratic form (36), which correspond to the two open channels. Secondly these channels have low density of states, i.e. low band curvature, as it can be confirmed using Fig. 4.

If the randomly distorted region is sufficiently long, the current decrease with the number of distorted cells can be approximated with exponential dependence $I[\varepsilon, N_D]$

$$I\left[\varepsilon, N_D\right] \approx I_{Ideal}\left[\varepsilon\right] Exp\left[-\frac{N_D}{N_L\left[\varepsilon\right]}\right] \tag{38}$$

Comparing the linear expansion of Eq.(38) with Eq.(36) one may deem that

$$N_L\left[\varepsilon\right] = I_{Ideal}\left[\varepsilon\right]\left(\frac{4e^2}{\pi\hbar}\sigma^2 \,\mathrm{Im}\left[\,\vec{J}\cdot B\cdot\vec{F}\,\right]\right)^{-1} . \quad \text{(WRONG)} \tag{39}$$

Equation (39), however, is incorrect, because during the derivation of Eqs.(36)-(37) we implied that electrons incoming towards the distorted region are equally distributed among all channels. This is not true if the distorted region is so long that the current exhibits exponential behavior (38). For that case the majority of incoming electrons belong to one conducting channel least susceptible to the influence of distortion. If this assumption is imposed on the derivation of Eqs.(36)-(37), matrix B has non-zero entries $B_{\alpha,\beta}$ only if either α or β correspond to the "best conducting channel", while $B_{\alpha,\beta}$ are still defined as $B_{\alpha,\beta} = |Vs_\alpha|^{-2}\ |Vs_\beta|^{-2}\, Cs_\alpha^{(Sq)} \cdot Cs_\beta^{(Sq)}$. Example below shows matrix B, which corresponds to four open channels, with channel 3 being the least susceptible to distortion:

$$B = \begin{pmatrix} B_{1,1} & B_{1,2} & B_{1,3} & B_{1,4} & 0 & \cdots \\ B_{2,1} & B_{2,2} & B_{2,3} & B_{2,4} & 0 & \cdots \\ B_{3,1} & B_{3,2} & B_{3,3} & B_{3,4} & 0 & \cdots \\ B_{4,1} & B_{4,2} & B_{4,3} & B_{4,4} & 0 & \cdots \\ 0 & 0 & 0 & 0 & 0 & \cdots \\ \vdots & \vdots & \vdots & \vdots & \vdots & \ddots \end{pmatrix} \rightarrow B' = \left(\begin{array}{cc|c|cc|c} 0 & 0 & B_{1,3} & 0 & 0 & \cdots \\ 0 & 0 & B_{2,3} & 0 & 0 & \cdots \\ \hline B_{3,1} & B_{3,2} & B_{3,3} & B_{3,4} & 0 & \cdots \\ \hline 0 & 0 & B_{4,3} & 0 & 0 & \cdots \\ 0 & 0 & 0 & 0 & 0 & \cdots \\ \vdots & \vdots & \vdots & \vdots & \vdots & \ddots \end{array}\right). \tag{40}$$

This model assumes that electrons from the most robust channel, which carries most of the current, can be scattered to all open channels, and vice versa; all other scattering processes are assumed to be negligible.

How do we find out, which channel is the most robust? The simplest, though not the fastest way, is to compute $\Delta I[\varepsilon]$ using Eq.(36) and Eq.(40) assuming in turn every open channel to be the best conducting channel. The channel, which corresponds to the smallest $\Delta I[\varepsilon]$ is the least sensitive to distortion.

It is possible to pick out the best conducting channel without testing every open channel. For open channels $|\Lambda s_\alpha| = 1$. The deviation of K_α from the real value due to the Hamiltonian distortion results in $|\Lambda s_\alpha| < 1$. Even a small shift of K_α into a complex plane may shut the channel off due to the large number of the distorted cells: $\left|\Lambda s_\alpha^{N_D}\right| << 1$. Thus, the best conducting channel must correspond to the lowest sensitivity of K_α to the Hamiltonian variation. A good measure of such sensitivity is the derivative $|\partial K_\alpha/\partial\varepsilon| = |Vs_\alpha^{-1}|$. The smallest $|Vs_\alpha^{-1}|$ guaranties that matrix B' defined by Eq.(40) is associated with the lowest $\Delta I[\varepsilon]$. Hence the localization length in terms of the number of unit cells is

$$N_L[\varepsilon] = I_{Ideal}[\varepsilon]\left(\frac{4e^2}{\pi\hbar}\sigma^2\,\mathrm{Im}\left[\vec{J}\cdot B'\cdot\vec{F}\right]\right)^{-1} . \tag{41}$$

$$B'_{\alpha,\beta} = |Vs_\alpha|^{-2}\ |Vs_\beta|^{-2}\ Cs_\alpha^{(Sq)}\cdot Cs_\beta^{(Sq)} \quad \text{if } |\Lambda s_\alpha| = 1 \text{ and } |\Lambda s_\beta| = 1$$
$$\text{and } |Vs_\alpha| = \mathrm{Max}[\{|Vs_\alpha|\}] \text{ or } |Vs_\beta| = \mathrm{Max}[\{|Vs_\alpha|\}]\ ; \tag{42}$$

$B_{\alpha,\beta} = 0$ otherwise. Plotted in Fig. 9 is $N_L[\varepsilon]$ computed using Eqs.(41)-(42) along the statistically computed $N_L^{(Stat)}[\varepsilon]$

$$N_L^{(Stat)}[\varepsilon] = N_0\left\langle Log\left[\frac{I_{Ideal}[\varepsilon]}{I[\varepsilon]}\right]\right\rangle^{-1} . \tag{43}$$

The averaging is performed over the ensemble of 750 distorted nano-tubes. Each nano-tube has $N_0 = 5000$ distorted cells, and the elements of δh are evenly distributed within the interval [-0.5 eV, +0.5 eV]. The single channel approximation works well when the number of channels is small, e.g. 2, 4, 6 in the three lowest conduction steps. In this case the differences between the channel susceptibilities to distortion are substantially large, and therefore for each energy there is well defined one robust channel. As the number of open channels increases the difference between them becomes less pronounced and two or more channels begin to compete for major current transport. Figure 10 contains the plots of Eq.(41) for all open channels, obtained by applying Eq.(40) to every open channel. The smaller is the difference between the best conducting channels, the least appro-

priate is the single channel approximation (41)-(42). Both analytical and statistical curves follow the same trend: localization length decreases with the increase of the state density and the number of open channels. Localization length has minima at the band edges.

IX. SUMMARY

We presented the non-recursive algorithm for computation of the self-energy accounting for the contacts with 1-D semi-infinite leads. The algorithm handles an arbitrary Hamiltonian types for leads with translational or screw symmetry. Analytic expression (7) results in the corollaries explaining convergence properties of the recursive relations (12), and the current dependence on the Green's function deviation (28), presented respectively in appendixes A and B. The analytic expressions for the current deviation (36) and localization length (41)-(42) are also based on the generalization of Eq.(7).

APPENDIX A

We prove that Eqs.(12) can be used for iterative computation of $\Sigma_L[\varepsilon]$ and $\Sigma_R[\varepsilon]$ only if either $\mathrm{Im}[\varepsilon] > 0$ or ε corresponds to zero density of states, i.e. lies within bandgap or outside spectral range of a lead. We prove this statement for $\Sigma_L[\varepsilon]$, the proof for $\Sigma_R[\varepsilon]$ is similar. The iterative relation for $\Sigma_L[\varepsilon]$ is

$$\Sigma_L^{(\mathrm{Out})} = \tau^T \cdot \left(\varepsilon\, I - h - \Sigma_L^{(\mathrm{In})}\right)^{-1} \cdot \tau \ . \tag{A1}$$

We assume that τ is non-singular. $\delta\Sigma_L{}^{(\mathrm{In})}$ and $\delta\Sigma_L{}^{(\mathrm{Out})}$ are respectively the deviations of $\Sigma_L{}^{(\mathrm{In})}$ and $\Sigma_L{}^{(\mathrm{Out})}$ from the true value Σ_L, which satisfies Eq.(A1). By using the first order expansion Eq.(A1) can be transformed to

$$\delta\Sigma_L^{(\mathrm{Out})} = -\tau^T \cdot \left(\varepsilon\, I - h - \Sigma_L\right)^{-1} \cdot \delta\Sigma_L^{(\mathrm{In})} \cdot \left(\varepsilon\, I - h - \Sigma_L\right)^{-1} \cdot \tau \ . \tag{A2}$$

Defining matrix $A \equiv \tau^{\mathrm{T}} \cdot (\varepsilon\, I - h - \Sigma_L)^{-1}$, Eq.(A2) can be rewritten in a compact form

$$\delta\Sigma_L^{(\mathrm{Out})} = -A \cdot \delta\Sigma_L^{(\mathrm{In})} \cdot A^T \ . \tag{A3}$$

Combining Eqs.(9-a) and (12-b) we obtain

$$A \equiv \tau^T \cdot \left(\varepsilon\, I - h - \Sigma_L\right)^{-1} = G_{0,0}^{-1} \cdot G_{1,0} \ . \tag{A4}$$

Since τ is assumed to be non-singular the contour contribution to the integral (17) vanishes and Eq.(19) can be applied to $G_{0,0}$. Similarly to Eq.(7-a)

$$G_{0,0}[\varepsilon] = -i\, CS \cdot VS^{-1} \cdot CS^T \ . \tag{A5}$$

For non-singular τ matrix CS is square and invertible. Combining Eqs.(7-a), (A4), and (A5) we obtain

$$A = -\left(CS^T\right)^{-1} \cdot \Lambda S \cdot CS^T \ . \tag{A6}$$

Hence the eigenvalues of A are the elements of the diagonal matrix ΛS. Equation (A3) can be rewritten in component form as

$$\left(\delta\Sigma_L^{(\mathrm{Out})}\right)_{i,j} = -\sum_{\alpha=1}^{N}\sum_{\beta=1}^{N} A_{i,\alpha} A_{j,\beta} \left(\delta\Sigma_L^{(\mathrm{In})}\right)_{\alpha,\beta} \ . \tag{A7}$$

One can view $\delta\Sigma_L{}^{(\mathrm{In})}$ and $\delta\Sigma_L{}^{(\mathrm{Out})}$ as the double-indexed vectors and $A_{i,\alpha}A_{j,\beta} \equiv a_{\{i,j\},\{\alpha,\beta\}}$ as the double indexed matrix, which is the direct product of matrixes A and A^{T}, i.e. $a = A \otimes A^{\mathrm{T}}$. The eigenvalues of the direct product is the set of all possible double products of

the constituent matrixes. That means the eigenvalues of a are all possible double products $\Lambda S_m \Lambda S_n = Exp[i(K_m + K_n)]$. For the convergence of iterative procedure (A7) the absolute values of all $Exp[i(K_m + K_n)]$ must be less than unity. Since all K_i are either real or belong to the upper complex half-plane the condition $| Exp[i(K_m + K_n)] | < 1 \ \forall K_i$ can be met only if $| Exp[i(K_m)] | < 1 \ \forall \ K_i$. That means all K_i must have positive imaginary part. If for certain real energy ε the is no single purely real K_i, no states are allowed for ε, i.e. energy ε lies outside spectral energy range or inside the bandgap. That completes the proof for non-singular τ. In the case when τ is singular, one applies the limiting procedure by using $\tau + \delta\tau$ instead of τ, where $\delta\tau$ is infinitesimally small non-singular matrix. In that case all finite eigenvalues are infinitesimally close to actual Λs_m, and fictitious infinitesimally small eigenvalues do not influence the convergence. That completes the proof.

APPENDIX B.

Current in 1-D systems. Quadratic dependence of the current deviation from the Green's function deviation.

In this Appendix we derive the expression for the current deviation from its ideal value. The problem setup is depicted in Fig.(B-1). We pick two adjacent supercells A and B lying to the right from the distorted region.

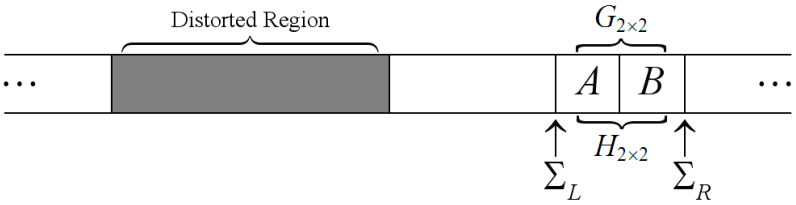

Figure B-1

Problem setup.

H_{Inf} and G_{Inf} are the Hamiltonian the Green's function for the entire (infinite) wire. Matrixes $H_{2\times2}$ and $G_{2\times2}[\varepsilon]$ are respectively the sub-blocks of H_{Inf} and G_{Inf} associated with AB segment:

$$G_{2\times2} = \begin{pmatrix} G_A & G_{BA}^T \\ G_{BA} & G_B \end{pmatrix}, \quad H_{2\times2} = \begin{pmatrix} h & \tau \\ \tau^T & h \end{pmatrix}. \tag{B1}$$

We also define matrixes

$$\tilde{\tau} = \begin{pmatrix} 0 & \tau \\ 0 & 0 \end{pmatrix}, \quad \Sigma L_{2\times2}[\varepsilon] = \begin{pmatrix} \Sigma_L[\varepsilon] & 0 \\ 0 & 0 \end{pmatrix}, \quad \Sigma R_{2\times2}[\varepsilon] = \begin{pmatrix} 0 & 0 \\ 0 & \Sigma_R[\varepsilon] \end{pmatrix}. \tag{B2}$$

where $\Sigma_L[\varepsilon]$, $\Sigma_L[\varepsilon]$, are self-energy matrixes of the same size as h and τ. The current corresponding to the particular energy ε in 1-D wire is[14]

$$I[\varepsilon] = -\frac{4e^2}{\pi\hbar}\mathrm{Tr}\left[\mathrm{Im}\left[G_{2\times2}[\varepsilon]\cdot\mathrm{Im}\left[\Sigma L_{2\times2}[\varepsilon]\right]\cdot G_{2\times2}^*[\varepsilon]\right]\cdot\tilde{\tau}\right]. \tag{B3}$$

Based on

$$G\cdot\mathrm{Im}[\Sigma_L]\cdot G^* = \mathrm{Im}[G] - G\cdot\mathrm{Im}[\Sigma_R]\cdot G^*. \tag{B4}$$

Eq.(B3) can be rewritten as

$$I = \frac{4e^2}{\pi\hbar}\mathrm{Tr}\Big[\,\mathrm{Im}\Big[G_{2\times2}\cdot\mathrm{Im}\big[\Sigma R_{2\times2}\big]\cdot G^{*}_{2\times2}\Big]\cdot\tilde{\tau}\Big]. \tag{B5}$$

Since we assume that there are no defects to the right from *AB*, $\Sigma R_{2\times2}$ corresponds to the ideal contact. To explicitly stress this fact, in the following we use $\Sigma RIdeal_{2\times2}$ instead of $\Sigma R_{2\times2}$. I_{Ideal} designates the current in the perfect wire

$$I_{Ideal} = \frac{4e^2}{\pi\hbar}\mathrm{Tr}\Big[\,\mathrm{Im}\Big[GIdeal_{2\times2}\cdot\mathrm{Im}\big[\Sigma RIdeal_{2\times2}\big]\cdot GIdeal^{*}_{2\times2}\Big]\cdot\tilde{\tau}\Big], \tag{B6}$$

where $GIdeal_{2\times2}$ is the sub-block of the ideal lead Green's function for two adjacent cells. As we prove in the following, **the difference I_{Ideal} - I is proportional to the square of the difference $GIdeal_{2\times2}$ - $G_{2\times2} \equiv \Delta G_{2\times2}$**:

$$I_{Ideal} - I = -\frac{4e^2}{\pi\hbar}\mathrm{Tr}\Big[\,\mathrm{Im}\Big[\Delta G_{2\times2}\cdot\mathrm{Im}\big[\Sigma RIdeal_{2\times2}\big]\cdot\Delta G^{*}_{2\times2}\Big]\cdot\tilde{\tau}\Big], \tag{B7}$$

while the terms linear in $\Delta G_{2\times2}$ are zero:

$$\begin{aligned}&\mathrm{Tr}\Big[\,\mathrm{Im}\Big[\Delta G_{2\times2}\cdot\mathrm{Im}\big[\Sigma RIdeal_{2\times2}\big]\cdot GIdeal^{*}_{2\times2}\Big]\cdot\tilde{\tau}\Big]+\\ &\mathrm{Tr}\Big[\,\mathrm{Im}\Big[GIdeal_{2\times2}\cdot\mathrm{Im}\big[\Sigma RIdeal_{2\times2}\big]\cdot\Delta G^{*}_{2\times2}\Big]\cdot\tilde{\tau}\Big]=0\ .\end{aligned} \tag{B8}$$

The proof of Eq.(B7) is equivalent to the proof of Eq.(B8), which can be rewritten as

$$\mathrm{Tr}\Big[\,\mathrm{Im}\Big[\Delta G_{2\times2}\cdot\mathrm{Im}\big[\Sigma RIdeal_{2\times2}\big]\cdot GIdeal^{*}_{2\times2}\Big]\cdot\big(\tilde{\tau}-\tilde{\tau}^{T}\big)\Big]\overset{?}{=}0\ . \tag{B9}$$

In transformation (B8) $\rightarrow$ (B9) we used the invariance of the trace under cyclic shifts and transposition. Before proceeding with the proof of (B9) we express $\Delta G_{2\times2}$ as

$$\begin{aligned}&\big(\varepsilon+i\eta\big)I_{2\times2}-H_{2\times2}-\Sigma RIdeal_{2\times2}-\Sigma L_{2\times2}=G^{-1}_{2\times2}\\ &\big(\varepsilon+i\eta\big)I_{2\times2}-H_{2\times2}-\Sigma RIdeal_{2\times2}-\Sigma LIdeal_{2\times2}=GIdeal^{-1}_{2\times2}\\ &\Downarrow\\ &\Sigma LIdeal_{2\times2}-\Sigma L_{2\times2}=G^{-1}_{2\times2}-GIdeal^{-1}_{2\times2}\\ &\Downarrow\\ &\Delta G_{2\times2}\equiv GIdeal_{2\times2}-G_{2\times2}=G_{2\times2}\cdot\big(\Sigma LIdeal_{2\times2}-\Sigma L_{2\times2}\big)\cdot GIdeal_{2\times2},\end{aligned} \tag{B10}$$

where $\Sigma LIdeal_{2\times2}$ is the self-energy of the ideal left contact. Denoting $T \equiv (\tilde{\tau}-\tilde{\tau}^{T})$ and substituting Eq.(B10) into Eq.(B9) we obtain

$$\mathrm{Tr}\Big[\,\mathrm{Im}\Big[\,G_{2\times2}\cdot\big(\Sigma LIdeal_{2\times2}-\Sigma L_{2\times2}\big)\cdot GIdeal_{2\times2}\cdot\mathrm{Im}\big[\Sigma RIdeal_{2\times2}\big]\cdot GIdeal^{*}_{2\times2}\,\Big]\cdot T\,\Big]=$$

$$\mathrm{Tr}\Big[\,\mathrm{Im}\Big[\big(\Sigma LIdeal_{2\times2}-\Sigma L_{2\times2}\big)\cdot GIdeal_{2\times2}\cdot\mathrm{Im}\big[\Sigma RIdeal_{2\times2}\big]\cdot GIdeal^{*}_{2\times2}\cdot T\cdot G_{2\times2}\,\Big]\Big]\overset{?}{=}0\,. \tag{B11}$$

The first two terms in the second line of Eq.(B11) can be represented as

$$\big(\Sigma LIdeal_{2\times2}-\Sigma L_{2\times2}\big)\cdot GIdeal_{2\times2}=\begin{pmatrix}\Sigma Ideal_L-\Sigma_L & 0\\ 0 & 0\end{pmatrix}\cdot GIdeal_{2\times2}\equiv\begin{pmatrix}a & b\\ 0 & 0\end{pmatrix}, \tag{B12}$$

where *a* and *b* are some matrixes, which structure is not important to us. Then Eq.(B11) is rewritten as

$$\mathrm{Tr}\left[\,\mathrm{Im}\left[\begin{pmatrix}a & b\\ 0 & 0\end{pmatrix}\cdot\mathrm{Im}\big[\Sigma RIdeal_{2\times2}\big]\cdot GIdeal^{*}_{2\times2}\cdot T\cdot G_{2\times2}\right]\right]\overset{?}{=}0\ . \tag{B13}$$

In the sub-block form Eq.(B13) is

$$\mathrm{Tr}\left[\,\mathrm{Im}\left[\begin{pmatrix}a & b\\ 0 & 0\end{pmatrix}\cdot\begin{pmatrix}0 & 0\\ 0 & \mathrm{Im}\big[\Sigma Ideal_R\big]\end{pmatrix}\cdot\begin{pmatrix}G^{*}_{0,0} & G^{*\,T}_{1,0}\\ G^{*}_{1,0} & G^{*}_{0,0}\end{pmatrix}\cdot\begin{pmatrix}0 & \tau\\ -\tau^{T} & 0\end{pmatrix}\cdot\begin{pmatrix}G_A & G^{T}_{BA}\\ G_{BA} & G_B\end{pmatrix}\right]\right]\overset{?}{=}0\,, \tag{B14}$$

which can be presented as

$$\mathrm{Tr}\Big[\,\mathrm{Im}\Big[\,b\cdot\mathrm{Im}\big[\Sigma Ideal_R\big]\cdot\big(G^{*}_{1,0}\cdot\tau\cdot G_{BA}-G^{*}_{0,0}\cdot\tau^{T}\cdot G_A\big)\Big]\Big]\overset{?}{=}0\,. \tag{B15}$$

From the identity

$$\begin{pmatrix}\big(\varepsilon+i\eta\big)I-h-\Sigma_L & -\tau\\ -\tau^{T} & \big(\varepsilon+i\eta\big)I-h-\Sigma Ideal_R\end{pmatrix}\cdot\begin{pmatrix}G_A & G^{T}_{BA}\\ G_{BA} & G_B\end{pmatrix}=I \tag{B16}$$

we obtain the expression for G_{BA} and G_A

$$\begin{aligned}G_A&=\big(\big(\varepsilon+i\eta\big)I-h-\Sigma_L-\Sigma Ideal_R\big)^{-1}\\ G_{BA}&=\big(\big(\varepsilon+i\eta\big)I-h-\Sigma Ideal_R\big)^{-1}\cdot\tau^{T}\cdot G_A\ .\end{aligned} \tag{B17}$$

Substituting Eq.(B17) into Eq.(B15) we obtain

$$\mathrm{Tr}\left[\,\mathrm{Im}\left[\,b\cdot\mathrm{Im}\big[\Sigma Ideal_R\big]\cdot\Big(G^{*}_{1,0}\cdot\tau\cdot\big(\big(\varepsilon+i\eta\big)I-h-\Sigma Ideal_R\big)^{-1}\cdot\tau^{T}-G^{*}_{0,0}\cdot\tau^{T}\Big)\cdot G_A\right]\right]\overset{?}{=}0\ . \tag{B18}$$

Using the recursive relation for $\Sigma Ideal_R$, Eq.(B18) can be transformed to

$$\mathrm{Tr}\Big[\,\mathrm{Im}\Big[\,b\cdot\mathrm{Im}\big[\Sigma Ideal_R\big]\cdot\big(G^{*}_{1,0}\cdot\Sigma Ideal_R-G^{*}_{0,0}\cdot\tau^{T}\big)\cdot G_A\Big]\Big]\overset{?}{=}0\ . \tag{B19}$$

The sufficient condition for the Eq.(B19) to be true is

$$\mathrm{Im}\left[\Sigma Ideal_R\right]\cdot\left(G_{1,0}\cdot\Sigma Ideal_R^{*}-G_{0,0}\cdot\tau^{T}\right)\overset{?}{=}0\ . \tag{B20}$$

Before we start the proof of Eq.(B20), we take closer look at the imaginary part of *G*. First we assume that τ is non-singular. That means Eq.(A5) is valid for $G_{0,0}$:

$$G_{0,0}[\varepsilon]=i\sum_{\alpha}\frac{Cs\left[K_\alpha\right]\cdot Cs\left[K_\alpha\right]^{T}}{-Vs\left[K_\alpha\right]}\ . \tag{B21}$$

Next we need to show that if Im[K_α] > 0, then for every such K_α exists -K_α^{*}, which also contributes to the sum (B21), and contribution from the pair K_α and -K_α^{*} is always real.

$$\begin{aligned}
&H\left[K_\alpha\right]=Exp\left[-i\,K_\alpha\right]\,\tau^{T}+h+Exp\left[i\,K_\alpha\right]\,\tau\\
&H\left[-K_\alpha^{*}\right]=H\left[K_\alpha\right]^{*}=Exp\left[i\,K_\alpha^{*}\right]\,\tau^{T}+h+Exp\left[-i\,K_\alpha^{*}\right]\,\tau\ .\\
&H\left[-K_\alpha^{*}\right]^{T}=H\left[K_\alpha\right]^{\dagger}
\end{aligned} \tag{B22}$$

By definition of $C\left[K_\alpha\right]$ and $\tilde{C}\left[K_\alpha\right]$

$$\begin{aligned}
&H\left[K_\alpha\right]\cdot C\left[K_\alpha\right]=\varepsilon\,C\left[K_\alpha\right]\\
&H\left[K_\alpha\right]^{T}\cdot\tilde{C}\left[K_\alpha\right]=\varepsilon\,\tilde{C}\left[K_\alpha\right]\ ,
\end{aligned} \tag{B23}$$

and

$$\begin{aligned}
&H\left[K_\alpha\right]^{*}\cdot C\left[K_\alpha\right]^{*}=\varepsilon^{*}\,C\left[K_\alpha\right]^{*}\\
&H\left[K_\alpha\right]^{\dagger}\cdot\tilde{C}\left[K_\alpha\right]^{*}=\varepsilon^{*}\,\tilde{C}\left[K_\alpha\right]^{*}\ .
\end{aligned} \tag{B24}$$

If ε is real,

$$C\left[K_\alpha\right]^{*}=C\left[-K_\alpha^{*}\right]\text{ and }\tilde{C}\left[K_\alpha\right]^{*}=\tilde{C}\left[-K_\alpha^{*}\right]. \tag{B25}$$

Therefore

$$\begin{aligned}
&V\left[K_\alpha\right]=i\,\tilde{C}\left[K_\alpha\right]\cdot\left(Exp\left[i\,K_\alpha\right]\,\tau-Exp\left[-i\,K_\alpha\right]\,\tau^{T}\right)\cdot C\left[K_\alpha\right]\\
&V\left[-K_\alpha^{*}\right]=-(-i)\tilde{C}\left[K_\alpha\right]^{*}\cdot\left(Exp\left[-i\,K_\alpha^{*}\right]\,\tau-Exp\left[i\,K_\alpha^{*}\right]\,\tau^{T}\right)\cdot C\left[K_\alpha\right]^{*}=-V\left[K_\alpha\right]^{*}
\end{aligned} \tag{B26}$$

Equations (B25) and (B26) indeed show that contribution from K_α and -K_α^{*} to Eq.(B21) is real:

$$i\frac{Cs\left[K_\alpha\right]\cdot Cs\left[K_\alpha\right]^{T}}{-Vs\left[K_\alpha\right]}+i\frac{Cs\left[-K_\alpha^{*}\right]\cdot Cs\left[-K_\alpha^{*}\right]^{T}}{-Vs\left[-K_\alpha^{*}\right]}=2\ \mathrm{Im}\left[i\frac{Cs\left[K_\alpha\right]\cdot Cs\left[K_\alpha\right]^{T}}{-Vs\left[K_\alpha\right]}\right]. \tag{B27}$$

Similarly the contribution from K_α and -K_α^{*} to $G_{1,0}$ is also real:

$$i\frac{Cs[K_\alpha]\cdot Cs[K_\alpha]^T}{-Vs[K_\alpha]}Exp[iK_\alpha]+i\frac{Cs[-K_\alpha^*]\cdot Cs[-K_\alpha^*]^T}{-Vs[-K_\alpha^*]}Exp[-iK_\alpha^*]= \\ 2\ \mathrm{Im}\left[i\frac{Cs[K_\alpha]\cdot Cs[K_\alpha]^T}{-Vs[K_\alpha]}Exp[iK_\alpha]\right]\ . \tag{B28}$$

Therefore the poles with non-zero Im[K_α], which appear in pairs do not contribute to the imaginary part of G. If Im[K_α] > 0, but Re[K_α] = 0, H[K_α] is real, and hence the eigen-vector C[K_α] is real, provided the corresponding eigenvalue ε is real. Therefore poles with Re[K_α] = 0 also do not contribute to the imaginary part of G. The same argument pertains to Re[K_α] = $\pm\pi$. Only the poles, which do not have symmetrical pairs, i.e. lying on the real axis, contribute to the imaginary part of the Green's function.

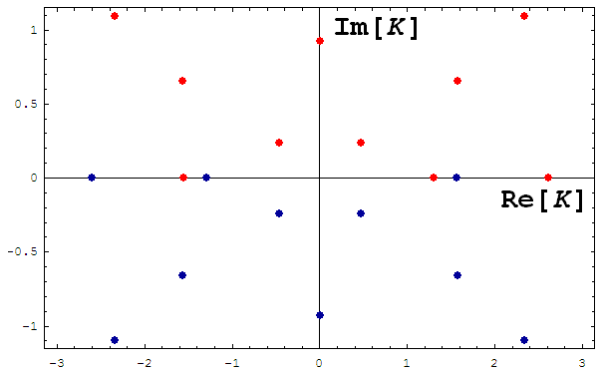

Figure 2

Poles K_α for randomly chosen h and τ. Red circles mark the poles which contribute to the sum (B21).

In the following we use matrixes CS, $\overline{CS}$, VS, and ΛS defined in section III, step 2. Additionally we assume that first M columns of CS and $\overline{CS}$, correspond to real K_α's. For convenience that will be obvious further all other $C[K_\alpha]$, and $\tilde{C}[K_\alpha]$ (except purely real $C[K_\alpha]$, and $\tilde{C}[K_\alpha]$ corresponding to Re[K_α] = 0, $\pm\pi$) are arranged in pairs: vectors $C[K_\alpha]$ and $C[-K_\alpha^*] = C[K_\alpha]^*$ stand together. Same for $\tilde{C}[K_\alpha]$ and $\tilde{C}[-K_\alpha^*]$. Since τ is assumed to be non-singular, the dimensions of matrixes CS, $\overline{CS}$, VS, and ΛS is $N\times N$.

Since τ is non-singular, the contour contribution to the integral (17) vanishes and Eq.(19) can be applied to $G_{0,0}$. Similarly to Eq.(7-a)

$$G_{0,0} = -i\ CS \cdot VS^{-1} \cdot CS^{T}, \tag{B29}$$

$$G_{1,0} = -i\ CS \cdot VS^{-1} \cdot \Lambda S \cdot CS^{T}, \tag{B30}$$

and hence

$$\begin{aligned} &\Sigma Ideal_R = G_{0,0}^{-1} \cdot G_{1,0}^{T} \cdot \tau^{T} = \Sigma Ideal_R^{T} = \tau \cdot G_{1,0} \cdot G_{0,0}^{-1} = \\ &\tau \cdot CS \cdot \Lambda S \cdot CS^{-1} = \left(CS^{T}\right)^{-1} \cdot \Lambda S \cdot CS^{T} \cdot \tau^{T} \ . \end{aligned} \tag{B31}$$

Here we used Eqs.(9-a,b), and the symmetry of self-energy matrix $\Sigma_{L,R} = \Sigma_{L,R}^{T}$. The latter follows from Eqs.(12-a,b) since $g_{0,0}$ is symmetric if energy and Hamiltonian are real. Now we return to the proof of Eq.(B20). First we are going to show that

$$CS^{T} \cdot \mathrm{Im}\left[\Sigma Ideal_R\right] = \begin{pmatrix} X & \cdots & \cdots & \cdots & \cdots & X \\ \vdots & \vdots & \vdots & \vdots & \vdots & \vdots \\ X & \cdots & \cdots & \cdots & \cdots & X \\ 0 & \cdots & \cdots & \cdots & \cdots & 0 \\ \vdots & \vdots & \vdots & \vdots & \vdots & \vdots \\ 0 & \cdots & \cdots & \cdots & \cdots & 0 \end{pmatrix}, \tag{B32}$$

where the number of non-zero rows (marked X) equals the number of real K_α's.

$$\begin{aligned} &CS^{T} \cdot \mathrm{Im}\left[\Sigma Ideal_R\right] = CS^{T} \cdot \mathrm{Im}\left[\left(CS^{T}\right)^{-1} \cdot \Lambda S \cdot CS^{T} \cdot \tau^{T}\right] = \\ &\frac{1}{2}\left\{CS^{T} \cdot \left(CS^{T}\right)^{-1} \cdot \Lambda S \cdot CS^{T} \cdot \tau^{T} - CS^{T} \cdot \left(CS^{\dagger}\right)^{-1} \cdot \Lambda S^{*} \cdot CS^{\dagger} \cdot \tau^{T}\right\} = \\ &\frac{1}{2}\left\{\Lambda S \cdot CS^{T} - CS^{T} \cdot \left(CS^{\dagger}\right)^{-1} \cdot \Lambda S^{*} \cdot CS^{\dagger}\right\} \cdot \tau^{T} \end{aligned} \tag{B33}$$

The product $CS^{T} \cdot (CS^{\dagger})^{-1}$ in the second term of Eq.(B33) is

$$CS^{T} \cdot \left(CS^{\dagger}\right)^{-1} = \begin{pmatrix} X & \cdots & \cdots & \cdots & \cdots & X \\ \vdots & \vdots & \vdots & \vdots & \vdots & \vdots \\ X & \cdots & \cdots & \cdots & \cdots & X \\ 0 & \cdots & 0 & \Xi & 0 & 0 \\ \vdots & \vdots & \vdots & 0 & \Xi & 0 \\ 0 & \cdots & 0 & 0 & 0 & \Xi \end{pmatrix}. \tag{B34}$$

Here X mark the elements of the first M non-zero rows, corresponding to real K_α's, and Ξ are 2×2 matrixes along main diagonal

$$\Xi = \begin{pmatrix} 0 & 1 \\ 1 & 0 \end{pmatrix}. \tag{B35}$$

The structure of the matrix (B34) can be easily understood if one takes into account that $(M + 1)^{\text{th}}$ row of CS^T and $(M + 2)^{\text{th}}$ row of $(CS^\dagger)^{-1}$ correspond to the same vector Cs_α. Therefore $(M + 1)^{\text{th}}$ and $(M + 2)^{\text{th}}$ rows of the product $CS^T \cdot (CS^\dagger)^{-1}$ have permuted 1's from the main diagonal. The same is true for all other pairs $\{K_\alpha, K_\alpha^*\}$ of complex K-vectors. Real Cs_α, if there are any, which represent $\mathrm{Re}[K_\alpha] = 0, \pm\pi$, do not have pairs. These vectors correspond to 1's on the main diagonal. Multiplication of the product $CS^T \cdot (CS^\dagger)^{-1}$ by the diagonal matrix ΛS^* does not change the structure of the matrix (B34)

$$CS^T \cdot \left(CS^\dagger\right)^{-1} \cdot \Lambda S^* = \begin{pmatrix} X & \cdots & \cdots & \cdots & \cdots & X \\ \vdots & \vdots & \vdots & \vdots & \vdots & \vdots \\ X & \cdots & \cdots & \cdots & \cdots & X \\ 0 & \cdots & 0 & \Omega & 0 & 0 \\ \vdots & \vdots & \vdots & 0 & \Omega & 0 \\ 0 & \cdots & 0 & 0 & 0 & \Omega \end{pmatrix}, \tag{B36}$$

where

$$\Omega = \begin{pmatrix} 0 & \Lambda_\alpha \\ \Lambda_\alpha^* & 0 \end{pmatrix}. \tag{B37}$$

Now, let us take a look at the last line in Eq.(B33). The first term in the curly brackets is the matrix $\Lambda S \cdot CS^T$, which rows are vectors Cs_α multiplied by the corresponding eigenvalues ΛS_α. The second term is $CS^T \cdot (CS^\dagger)^{-1} \cdot \Lambda S^* \cdot CS^\dagger$. The last $N - M$ rows of matrix $CS^\dagger$ are the permuted pairs of the rows of matrix CS^T. The multiplication of such a pair in $CS^\dagger$ by Ω constitutes the second permutation, which restores the order in the pair. That makes the last $N - M$ rows of the matrixes $\Lambda S \cdot CS^T$ and $CS^T \cdot (CS^\dagger)^{-1} \cdot \Lambda S^* \cdot CS^\dagger$ identical:

$$\Lambda S \cdot CS^T - CS^T \cdot \left(CS^\dagger\right)^{-1} \cdot \Lambda S^* \cdot CS^\dagger = \begin{pmatrix} X & \cdots & \cdots & \cdots & \cdots & X \\ \vdots & \vdots & \vdots & \vdots & \vdots & \vdots \\ X & \cdots & \cdots & \cdots & \cdots & X \\ 0 & \cdots & \cdots & \cdots & \cdots & 0 \\ \vdots & \vdots & \vdots & \vdots & \vdots & \vdots \\ 0 & \cdots & \cdots & \cdots & \cdots & 0 \end{pmatrix} . \tag{B38}$$

That completes the proof of Eq.(B32). We use Eqs.(B29-31) to transform Eq.(B20) as

$$\begin{aligned} &\mathrm{Im}\left[\Sigma Ideal_R\right] \cdot \left(G_{1,0} \cdot \Sigma Ideal_R^* - G_{0,0} \cdot \tau^T\right) = \\ &-i \;\; \mathrm{Im}\left[\Sigma Ideal_R\right] \cdot CS \cdot VS^{-1} \cdot \left(\Lambda S \cdot CS^T \cdot \Sigma Ideal_R^* - CS^T \cdot \tau^T\right) = \\ &-i \;\; \mathrm{Im}\left[\Sigma Ideal_R\right] \cdot CS \cdot VS^{-1} \cdot \left(\Lambda S \cdot CS^T \cdot \left(CS^\dagger\right)^{-1} \cdot \Lambda S^* \cdot CS^\dagger - CS^T\right) \cdot \tau^T \stackrel{?}{=} 0 \end{aligned} \tag{B39}$$

The factor $\mathrm{Im}[\Sigma Ideal_R^*] \cdot CS$ in Eq.(B39) is the transposed Eq.(B32). The diagonal matrix VS^{-1} does not change the structure of Eq.(B32)

$$\mathrm{Im}\left[\Sigma Ideal_R\right] \cdot CS \cdot VS^{-1} = \begin{pmatrix} X & \cdots & X & 0 & \cdots & 0 \\ \vdots & \cdots & \vdots & \vdots & \cdots & \vdots \\ \vdots & \cdots & \vdots & \vdots & \cdots & \vdots \\ \vdots & \cdots & \vdots & \vdots & \cdots & \vdots \\ \vdots & \cdots & \vdots & \vdots & \cdots & \vdots \\ X & \cdots & X & 0 & \cdots & 0 \end{pmatrix} . \tag{B40}$$

Since the first M rows of CS^T are real they are identical to the first M rows of $CS^\dagger$. Hence the product in the first term in the parenthesis in Eq.(B39) is

$$\Lambda S \cdot CS^T \cdot \left(CS^\dagger\right)^{-1} \cdot \Lambda S^* = \begin{pmatrix} 1 & 0 & 0 & \cdots & \cdots & 0 \\ 0 & 1 & 0 & \vdots & \vdots & \vdots \\ 0 & 0 & 1 & \cdots & \cdots & 0 \\ X & \cdots & \cdots & \cdots & \cdots & X \\ \vdots & \vdots & \vdots & \vdots & \vdots & \vdots \\ X & \cdots & \cdots & \cdots & \cdots & X \end{pmatrix} . \tag{B41}$$

Therefore the entire term in the parenthesis has the form

$$\Lambda S \cdot CS^T \cdot \left(CS^\dagger\right)^{-1} \cdot \Lambda S^* \cdot CS^\dagger - CS^T = \begin{pmatrix} 0 & \cdots & \cdots & \cdots & \cdots & 0 \\ \vdots & \vdots & \vdots & \vdots & \vdots & \vdots \\ 0 & \cdots & \cdots & \cdots & \cdots & 0 \\ X & \cdots & \cdots & \cdots & \cdots & X \\ \vdots & \vdots & \vdots & \vdots & \vdots & \vdots \\ X & \cdots & \cdots & \cdots & \cdots & X \end{pmatrix} . \qquad \text{(B42)}$$

Multiplication of the matrixes (B40) and (B42) is zero:

$$\begin{pmatrix} X & \cdots & X & 0 & \cdots & 0 \\ \vdots & \cdots & \vdots & \vdots & \cdots & \vdots \\ \vdots & \cdots & \vdots & \vdots & \cdots & \vdots \\ \vdots & \cdots & \vdots & \vdots & \cdots & \vdots \\ \vdots & \cdots & \vdots & \vdots & \cdots & \vdots \\ X & \cdots & X & 0 & \cdots & 0 \end{pmatrix} \cdot \begin{pmatrix} 0 & \cdots & \cdots & \cdots & \cdots & 0 \\ \vdots & \vdots & \vdots & \vdots & \vdots & \vdots \\ 0 & \cdots & \cdots & \cdots & \cdots & 0 \\ X & \cdots & \cdots & \cdots & \cdots & X \\ \vdots & \vdots & \vdots & \vdots & \vdots & \vdots \\ X & \cdots & \cdots & \cdots & \cdots & X \end{pmatrix} = 0 \quad . \qquad \text{(B43)}$$

That completes the proof of Eq.(B20) for non-singular τ. In the case when τ is singular, one applies the limiting procedure by using $\tau + \delta\tau$ instead of τ, where $\delta\tau$ is a small non-singular matrix. In the limit $\delta\tau \to 0$ all actual eigenvalues and eigenvectors are infinitesimally close to respective Λs_α and Cs_α, while fictitious infinitesimally small eigenvalues and corresponding eigenvectors do not affect the course of the proof. That completes the proof of Eq.(B20) and hence Eq.(B7).

FIGURES

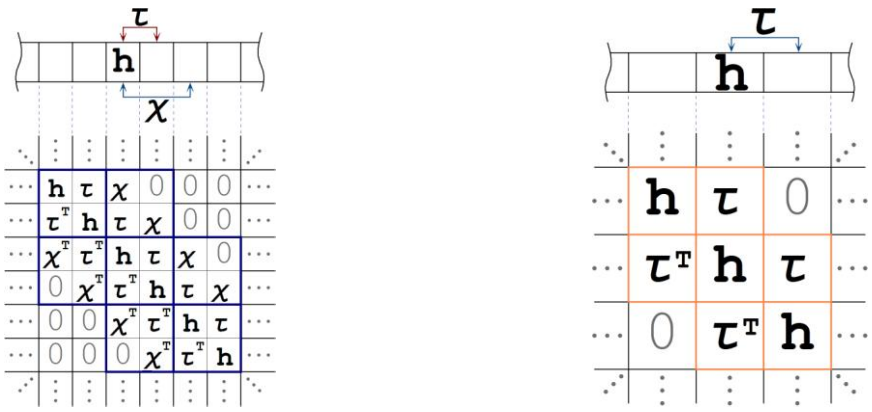

Figure 1

Normalizing Hamiltonian to the tri-block-diagonal form. **(a)** Translationally periodic infinite lead (top) and the infinite block-band Hamiltonian in the second neighbor approximation associated with the lead. τ and χ are the coupling matrices to the first and second unit cell neighbors respectively. **(b)** The increase of the unit cell size eliminates the interaction beyond the first nearest neighbor, and "transforms" Hamiltonian to the tri-block-diagonal structure.

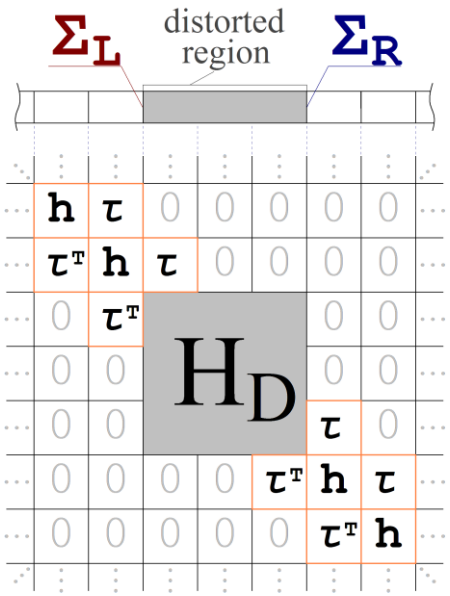

Figure 2

Illustration to definition of Σ_L and Σ_R. The infinite lead containing defective region three unit cells long (upper portion), and the corresponding Hamiltonian matrix.

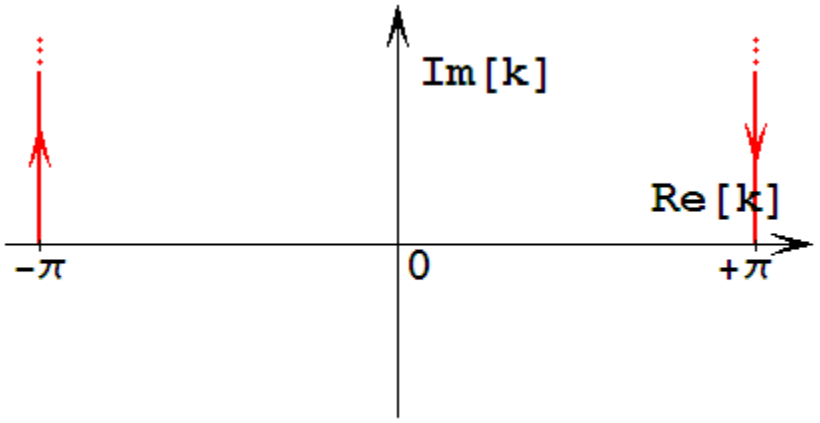

Figure 3

Contour for complex *K*-plane integration.

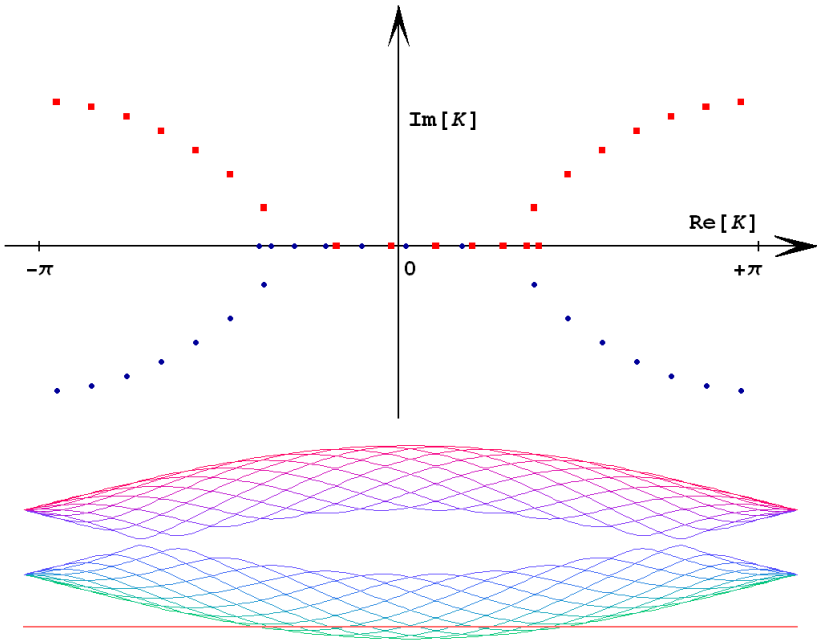

Figure 4

Poles positions for (11, 10) nano-tube. Squares mark the poles, which contribute to the contour integral. Poles are computed for the nearest neighbor π-orbital tight-binding model. Bottom portion of the figure contains the nano-tube band-structure plot. Horizontal line marks the energy ε = -7.12345 eV, for which the poles have been computed. The loci of the poles for a certain energy range constitute the so called "real energy lines", which can be also viewed as complex *K* band-structure.

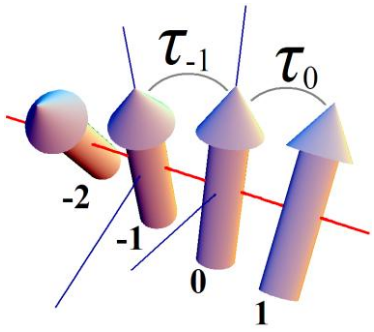

Figure 5

Schematic illustration of 1-D system with screw symmetry. Matrix τ_0 couples cells with indexes 0 and 1; τ_{-1} couples cells with indexes -1 and 0. τ_{-1} is identical to τ_0 in the coordinate system attached to the cell with index –1: $\tau_{-1} = R^{-1} \cdot \tau_0 \cdot R$. Here R is the orbital rotation matrix associated with the screw angle.

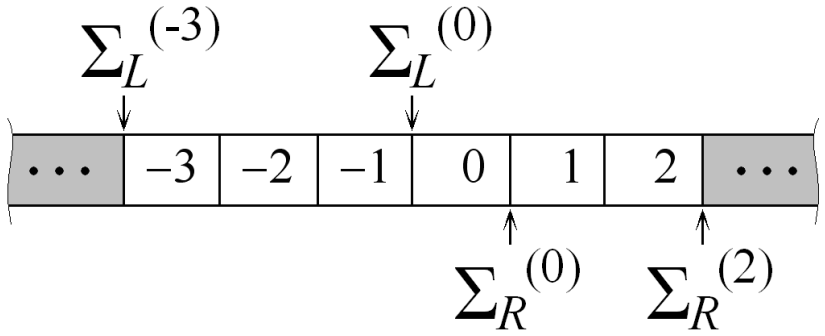

Figure 6

Self-energy transformation example for the system with screw symmetry. $\Sigma_L^{(-3)}$ and $\Sigma_R^{(2)}$ account for the contacts represented by the shaded areas, while $\Sigma_L^{(0)}$ and $\Sigma_R^{(0)}$ are generated by the algorithm descried in section III, provided the substitution $\tau \rightarrow \tau \cdot R$ is made. $\Sigma_L^{(-3)} = R^{-3} \cdot \Sigma_L^{(0)} \cdot R^3$ and $\Sigma_R^{(2)} = R^2 \cdot \Sigma_R^{(0)} \cdot R^{-2}$.

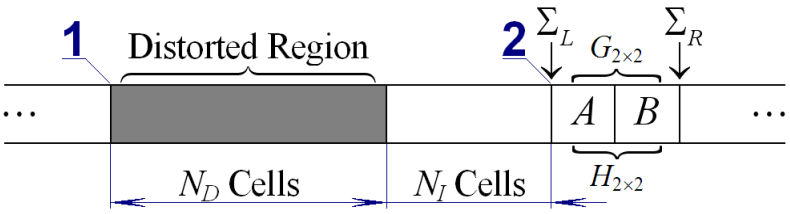

Figure 7

Problem setup for current calculation.

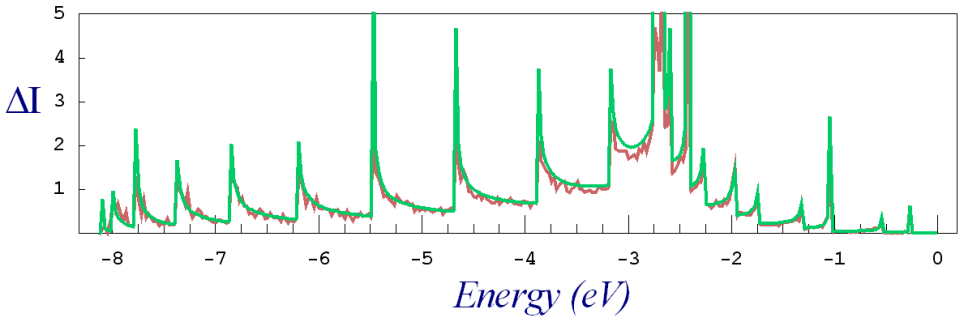

Figure 8

ΔI for (11,10) nano-tube. The smooth (green) line corresponds to Eqs.(36)-(37). Rough (brown) line was obtained through direct simulation for the given random defect distribution by "growing" the defective region through the recursive computation of the self-energy.

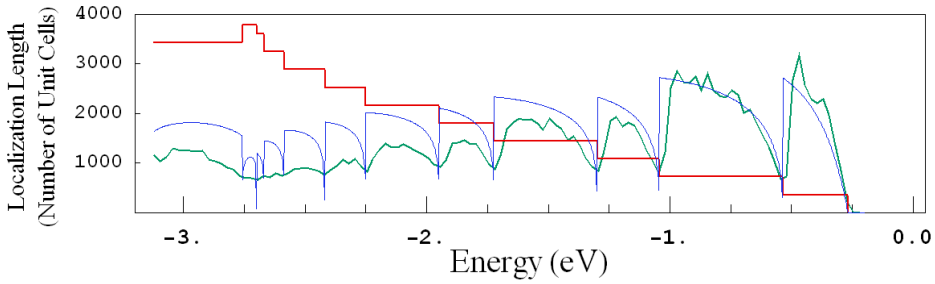

Figure 9

Localization length as a function of energy for (11,10) nano-tube. Smooth line corresponds to the analytic expressions (41)-(42), rough line is obtained using statistical averaging. $I_{Ideal}[\varepsilon]$ is plotted for reference in arbitrary units.

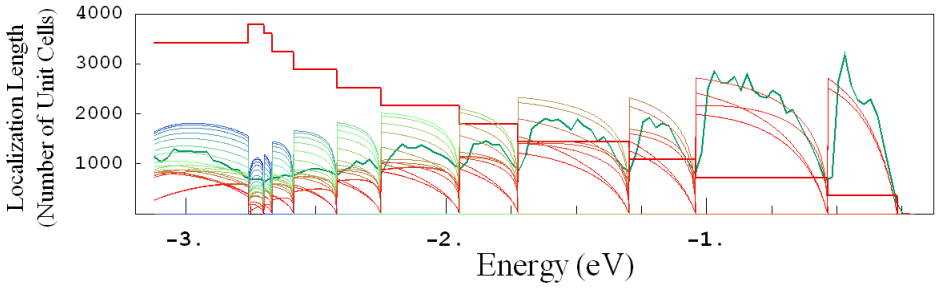

Figure 10

Localization length for (11,10) nano-tube measured in numbers of unit-cells. Thin smooth lines correspond to the analytic expressions (41)-(42) applied in turn for all open channels. Rough line corresponds to the localization length obtained through the statistical averaging. Thick red line is $I_{Ideal}[\varepsilon]$ plotted for reference in arbitrary units.

REFERENCES:

[1] A. Pecchia, A. Di Carlo, ”Atomistic theory of transport in organic and inorganic nanostructures”, Reports on Progress in Physics **67**, 1497 (2004).

[2] J. Velev and W. Butler, “On the equivalence of different techniques for evaluating the Green function for a semi-infinite system using a localized basis”, J. Phys.: Condens. Matter **16**, R637 (2004).

[3] M.P. Lopez Sancho, J.M. Lopez Sancho, J. Rubio, “Highly convergent schemes for the calculation of bulk and surface Green’s functions”, J. Phys. F: Met. Phys. **15**, 851 (1985)

[4] S.Y. Wu, J. Cocks, C. S. Jayanthi, Phys. Rev. B **49**, 7957 (1994).

[5] M. Galperin, S. Toledo, A. Nitzan, “Numerical computation of tunneling fluxes” J. Chem. Phys. **117**, 10817 (2002).

[6] A. Umerski, “Closed-form solutions to surface Green's functions”, Phys. Rev. B **55**, 5266 (1997).

[7] K.S. Dy, S.-Y. Wu, T. Spratlin, Phys. Rev. B **20**, 4237 (1979).

[8] R.E. Allen, Phys. Rev. B, **19**, 917 (1979); **20**, 1454 (1979).

[9] D.H. Lee, J.D. Joannopoulos, “Simple scheme for surface-band calculations. 2. The Green’s-function.”, Phys. Rev. B **23**, 4997 (1981).

[10] Yia-Chung Chang and J.N. Schulman, Phys. Rev. B, **25**, 3975, (1981).

[11] J.T. Tomfohr and O.F. Sankey, Phys. Rev. B, **65**, 245105, (2002).

[12] S. Datta, “Electronic transport in mesoscopic systems”, Cambridge University Press (1995), Chapter 5.

[13] M. Brandbyge, J.-L. Mozos, P. Ordejon, J. Taylor, and K. Stokbro, “Density-functional method for nonequilibrium electron transport”, Phys. Rev. B **65**, 165401 (2002).

[14] S. Datta, “Nanoscale device modeling: the Green’s function method”, Superlatt. Microstruct. **28** 253 (2000).

[15] T.N. Todorov, “Tight-binding simulation of current carrying nanostructures”, J. Phys.: Condens. Matter **14**, 3049 (2002).